# Langevin approach for the dynamics of the contact process on annealed scale-free networks

Marián Boguñá,[1] Claudio Castellano,[2] and Romualdo Pastor-Satorras[3]
[1]*Departament de Física Fonamental, Universitat de Barcelona, Martí i Franquès 1, 08028 Barcelona, Spain*
[2]*SMC, INFM-CNR, and Dipartimento di Fisica, "Sapienza" Università di Roma, Piazzale Aldo Moro 2, I-00185 Roma, Italy*
[3]*Departament de Física i Enginyeria Nuclear, Universitat Politècnica de Catalunya, Campus Nord B4, 08034 Barcelona, Spain*
(Received 16 October 2008; published 19 March 2009)

We study the dynamics of the contact process, one of the simplest nonequilibrium stochastic processes, taking place on a scale-free network. We consider the network topology as annealed, i.e., all links are rewired at each microscopic time step, so that no dynamical correlation can build up. This is a practical implementation of the absence of correlations assumed by mean-field approaches. We present a detailed analysis of the contact process in terms of a Langevin equation, including explicitly the effects of stochastic fluctuations in the number of particles in finite networks. This allows us to determine analytically the survival time for spreading experiments and the density of active sites in surviving runs. The fluctuations in the topological structure induce anomalous scaling effects with respect to the system size when the degree distribution has a hard upper bound. When the upper bound is soft, the presence of outliers with huge connectivity perturbs the picture even more, inducing an apparent shift of the critical point. In light of these findings, recent theoretical and numerical results in the literature are critically reviewed.

DOI: 10.1103/PhysRevE.79.036110 PACS number(s): 89.75.Hc, 05.70.Jk, 05.10.Gg, 64.60.an

## I. INTRODUCTION

The study of the effects of a heterogeneous topology on equilibrium and nonequilibrium dynamical processes has lately experienced active interest from the statistical physics community [1]. Indeed, it has been observed in recent years that many natural and man-made systems are well characterized in terms of complex networks or graphs [2,3], in which vertices represent elementary units in the system, while edges stand for pairwise interactions between elements. Most real networked systems can be characterized by a heterogeneous complex topology, showing remarkable universal features, such as the small-world property [4] and a scale-free connectivity pattern [5]. The small-world property refers to the fact that the average distance $\langle \ell \rangle$ between any two vertices—defined as the smallest number of edges on a path between one and the other—is very small, scaling logarithmically or even more slowly with the network size $N$ [6]. This is to be compared to the power-law scaling $\langle \ell \rangle \sim N^{1/d}$ in a $d$-dimensional lattice. Since the logarithm grows more slowly than any power-law function, even if $d$ is very large, small-world networks can be thought of as highly compact objects of infinite dimensionality. On the other hand, scale-free (SF) networks are typically characterized by a degree distribution $P(k)$, defined as the probability that a randomly selected vertex has degree $k$—is connected to $k$ other vertices—that decreases as a power law,

$$P(k) \sim k^{-\gamma}, \tag{1}$$

where $\gamma$ is a characteristic degree exponent, usually in the range $2 < \gamma \leqslant 3$ [2,3].

Dynamical processes taking place on top of complex networks arise in a wide variety of scientific and technological contexts. For example, we can mention the transmission of information packets on the internet [7], the spreading of biological diseases on social networks or computer viruses in computer infrastructures [8,9], etc. The interest in the study of these dynamics was triggered by the observation that the heterogeneous connectivity pattern observed in SF networks with diverging degree fluctuations can lead to very surprising outcomes, such as an extreme weakness in the face of targeted attacks aimed at destroying the most connected vertices [10,11], or the ease of propagation of infective agents [9,12]. These properties are due to the critical interplay between topology and dynamics in heterogeneous networks and are absent in their homogeneous counterparts. After those initial discoveries, a real avalanche of new results have been put forward, including classical equilibrium systems [13–15] and nonequilibrium processes such as epidemic spreading [9,12], reaction-diffusion processes [16–18], and dynamics with absorbing states [19,20]. For an extensive review of recent results, we refer the reader to Ref. [1].

The analytical approach to the study of dynamical processes on complex networks is dominated by the application of heterogeneous mean-field theory [1]. Heterogeneous mean-field (HMF) theory is based on two basic assumptions: (i) the homogeneous mixing hypothesis, stating that all vertices with the same degree (within the same degree class) share the same dynamical properties; and (ii) the assumption that fluctuations are not relevant, and therefore analytical studies can be conducted within a deterministic approach. This last fact is in some sense natural, since the small-world property implies that dynamical fluctuations in a network are so close together that they can be washed away in very few time steps.[1] HMF has proved to be extremely useful in providing a very accurate description of the behavior of most dynamical processes on complex networks [1]. On the other hand, in other instances, such as in the nonequilibrium contact process (CP) [22] a debate has arisen about the comparison between numerical simulations on SF networks and

[1]This is at variance with what happens in regular lattices below the critical dimension, where in particular, close to a critical point, the dynamics is governed by fluctuations [21].

 

HMF predictions [19,23,24]. Underlying this controversy is the fact that while the HMF approach considers all relevant quantities as deterministic, and hence assumes an infinite system size, numerical simulations are performed on finite systems and thus are necessarily influenced by stochastic fluctuations due to the finite number of particles, in particular close to an absorbing state phase transition [22]. Finite-size effects are very strong in networks and an appropriate theoretical framework for them is necessary to compare simulations with HMF results. For this reason, in Ref. [25] the CP was considered on the simplest network substrate, which is an annealed network, in which the quenched disorder imposed by the actual connections in the network is not considered. In this scenario, it was possible to deduce, by means of qualitative arguments, the correct size scaling of the CP in this kind of network, in very good agreement with numerical simulations.

In this paper we present a more detailed analysis of the CP in SF networks, deriving the corresponding Langevin equation describing its dynamics for the case of annealed networks. The analysis of this equation allows us to uncover the correct finite-size scaling behavior of the CP in heterogeneous networks, providing the exact value of the critical exponents describing this system. Surprisingly, the critical behavior of the CP turns out to be extremely sensitive to the particular degree cutoff chosen for the construction of the network, in agreement with previous results obtained from a more phenomenological approach [25]. In particular, critical exponents depend explicitly on the way the degree cutoff diverges with the system size, if it scales sufficiently slowly. If the scaling is instead fast, additional complications arise and fluctuations of the degree distribution strongly perturb the picture.

We have organized our paper as follows. In Sec. II we describe the main properties of annealed networks, which represent the simplest network substrate for a dynamical process, in which mean-field theory is supposed to be exact. We focus, in particular, on the effects of the maximum degree allowed on the network cutoff and on its fluctuations. Section III defines the CP on complex networks, whose mean-field analysis is reviewed in Sec. IV. In Sec. V we comment on the different approaches followed in the past to deal with finite-size effects on the CP in SF networks. The general Langevin theory for the CP in networks is presented in Sec. VI, while Sec. VII focuses on the analysis of annealed networks. Section VIII discusses the meaning of finite-size effects and finite-size scaling in heterogeneous networks. In Sec. IX we present a digression to the case of annealed networks with outliers, that is, vertices with a degree much larger than the average maximum degree expected in the network. Finally, we draw our conclusions in Sec. X. Some technical questions are developed in several Appendixes.

## II. ANNEALED SCALE-FREE NETWORKS

The topological properties of any complex network are fully encoded in its adjacency matrix $a_{ij}$, taking the value $a_{ij}=1$ if there is an edge connecting vertices $i$ and $j$, and zero otherwise. In so-called *quenched networks*, the values of the adjacency matrix are fixed in time. For large quenched networks, a statistical characterization in terms of the degree distribution $P(k)$ and the degree correlations $P(k'|k)$, defined as the conditional probability that a vertex of degree $k$ is connected to a vertex of degree $k'$ [26,27], is useful as a compact way to express the essential features of the adjacency matrix.[2] Quenched networks are the typical output of most network models, such as the configuration model [28–31], the uncorrelated configuration model [32], the class of models with hidden variables [33], linear preferential attachment models [5,34], etc. In this case, each network must be considered as a representative of a statistical ensemble of random networks, which is characterized by the $P(k)$ and $P(k'|k)$ probability distributions. When a dynamical process takes place on top of such a network, one is considering the network as frozen, with respect to the characteristic time scale $\tau_D$ of the dynamics. In this case, in a numerical analysis of a dynamical process, one must consider the dynamics over many different quenched networks, all belonging to the network ensemble with the same statistically equivalent topological properties, and perform an ensemble average to compute the average dynamical quantities.

In other instances, on the other hand, the very network is a dynamical object, changing in time over a certain time scale $\tau_N$. In this case, the correct topological characterization is strictly statistical, given in terms of the degree distribution $P(k)$ and the degree correlations $P(k'|k)$. In the limit $\tau_N \ll \tau_D$, that is, when the network connections are completely reshuffled between any two microscopic steps of the dynamics, while keeping fixed $P(k)$ and $P(k'|k)$, the resulting networks are called *annealed* [35–37] (see also the interesting case of blinking networks [38]). Apart from the cases where they describe the actual evolution of real systems, annealed networks are extremely important from a theoretical point of view, because mean-field predictions for dynamical processes on networks are usually obtained in this limit, via the so-called annealed network approximation [1]. In practice one replaces the adjacency matrix $a_{ij}$ by its ensemble average $\bar{a}(k_i,k_j)$, defining the probability that two vertices of degree $k_i$ and $k_j$ are connected. This average is given by

$$\bar{a}(k,k') = \frac{1}{NP(k)}\frac{1}{NP(k')}\sum_{i\in k}\sum_{j\in k'} a_{ij} \equiv \frac{k'P(k|k')}{NP(k)}, \qquad (2)$$

where the notation $i \in k$ means summation for all vertices of degree $k$. Taking the case of uncorrelated networks, with $P(k|k')=kP(k)/\langle k\rangle$ [39], the simple form $\bar{a}(k,k')=kk'/N\langle k\rangle$ results.

From a numerical point of view, the simulation of dynamics on annealed networks implies the regeneration of the whole network every time a microscopic dynamic step is performed [37]. For uncorrelated networks this can be efficiently implemented in CP-like dynamics. In this case, an annealed network of size $N$ is completely defined by its degree sequence $\{k_1,\ldots,k_N\}$, where the degrees $k_i$ are integer random numbers, extracted according to the degree distribu-

[2] A more detailed characterization can be made using higher-order degree correlations; see Ref. [27].

tion $P(k)$, and restricted between a lower bound $m$ and an upper bound $M \leqslant N$. Degree correlations are given by $P(k'|k)=k'P(k')/\langle k\rangle$. Thus, every time we need to find a nearest neighbor of a vertex, it is selected at random with probability $k'P(k')/\langle k\rangle$ among the $N$ vertices present in the network. This procedure ensures a complete lack of dynamical correlations between vertices, except in rare events in which a vertex chooses itself as a nearest neighbor, an event that happens with probability $k/N$ for vertices of degree $k$. This probability is, however, vanishingly small in the limit of large networks (see below).

Finite SF networks are additionally characterized by another parameter, the degree cutoff $k_c(N)$ [39], which is the average value of the actual maximum degree $k_{\max}$ in a single realization of the degree sequence: $k_c(N)=\langle k_{\max}\rangle$. In general, $k_c$ is a nondecreasing function of the network size and, as we shall see below, the CP dynamics is very sensitive to its actual size dependence.

Notice that the value of the cutoff plays a relevant role in the determination of degree correlations in finite quenched networks [40]. It is known that for the network to be closed without degree-degree correlations and no multiple edges or self-loops one must impose the requirement that degrees are smaller than the *structural* cutoff $\sim N^{1/2}$ [32]. In uncorrelated annealed networks, however, since they are by construction uncorrelated, such a restriction does not apply, and any cutoff is in principle possible.

Simple considerations based on extreme value theory [40] give the probability distribution $P_{\max}(k_{\max})$ of observing a maximum degree $k_{\max}$ among $N$ degrees independently sampled from a distribution $P(k)\sim k^{-\gamma}$ and bounded by the constraint $m \leqslant k \leqslant M$. In the continuous degree approximation, the distribution of maximum degrees takes the form

$$P_{\max}(k_{\max}=k)=N(\gamma-1)\frac{(m^{1-\gamma}-k^{1-\gamma})^{N-1}}{(m^{1-\gamma}-M^{1-\gamma})^{N}}k^{-\gamma}. \tag{3}$$

The derivation of this expression is based on extreme value theory. Following Ref. [40], the distribution function of the event that the maximum degree is smaller than or equal to $k$, $\Pi_{\max}(k_{\max}\leqslant k)$ is given by

$$\Pi_{\max}(k_{\max}\leqslant k)=\left(\int_m^k P(k')dk'\right)^N, \tag{4}$$

corresponding to the probability of all vertices having degree at most $k$. The density function will then be given by

$$P_{\max}(k_{\max}=k)=\frac{d}{dk}\Pi_{\max}(k_{\max}\leqslant k), \tag{5}$$

which yields Eq. (3), provided we use the normalized degree distribution $P(k)=(\gamma-1)(m^{-\gamma+1}-M^{-\gamma+1})^{-1}k^{-\gamma}$. Using Eq. (3) one can compute explicitly the value of $k_c(N)$, obtaining two different behaviors, depending on whether $M/m$ is larger or smaller than $N^{1/(\gamma-1)}$, namely,

$$k_c(N)=\begin{cases} M, & \dfrac{M}{m}\ll N^{1/(\gamma-1)}, \\ m\Gamma\left(\dfrac{\gamma-2}{\gamma-1}\right)N^{1/(\gamma-1)}, & \dfrac{M}{m}\gg N^{1/(\gamma-1)}, \end{cases} \tag{6}$$

where $\Gamma(z)$ is the Gamma function [41].

For the network to be SF the upper bound of the degree distribution must diverge with the system size: $M\sim N^{1/\omega}$. The parameter $\omega\geqslant 0$ is in principle arbitrary, but its value strongly affects the nature of the actual maximum of the degree sequence. If $M$ diverges not faster than $N^{1/(\gamma-1)}$ (i.e., $\omega\geqslant\gamma-1$), then $k_c=M$ is a hard cutoff, with no degree larger than $k_c$. For $\omega<\gamma-1$ instead, $k_c\sim N^{1/(\gamma-1)}$ is just an average cutoff, but $\langle k_{\max}^2\rangle$ grows with the network size as $N^{1+(3-\gamma)/\omega}\gg k_c^2$, indicating that fluctuations diverge.

As a consequence, the maximum degree present in the degree sequence has wide fluctuations, and *outliers*, i.e., nodes with a degree much larger than $k_c$, may be present in the network. It is important to stress that taking $\omega=\gamma-1$ is very different from setting $M=\infty$ from the beginning ($\omega=0$) or $M=N$ ($\omega=1$), as is usually done in the quenched configuration model [31]. In both cases the average cutoff $k_c$ scales as $N^{1/(\gamma-1)}$, but for $\omega=\gamma-1$ this is a hard cutoff and fluctuations of the value of $k_{\max}$ around $k_c$ are bounded.

The presence of outliers and large fluctuations in the maximum degree has a strong effect on the dynamics on annealed networks. In particular, as we will see, the relevant quantity characterizing the size effects on the dynamics is the second moment of the degree distribution,

$$g=\frac{\langle k^2\rangle}{\langle k\rangle^2}. \tag{7}$$

The fluctuating nature of this quantity from sample to sample can be assessed by looking at its standard deviation $\sigma_g$, which can be easily computed, given the uncorrelated nature of the degrees in annealed networks. Thus, we have the relative fluctuations

$$\frac{\sigma_g^2}{g^2}=\frac{1}{N}\left(\frac{\langle k^4\rangle}{\langle k^2\rangle^2}-1\right). \tag{8}$$

Assuming that $\langle k^n\rangle\sim\langle {k_{\max}}^{n+1-\gamma}\rangle$, we have

$$\frac{\sigma_g^2}{g^2}\sim\frac{\langle {k_{\max}}^{5-\gamma}\rangle}{N\langle {k_{\max}}^{3-\gamma}\rangle^2}\sim\begin{cases} N^{2(3-\gamma)[1/\omega-1/(\gamma-1)]} & \text{for } \omega<\gamma-1, \\ N^{(\gamma-1)/\omega-1} & \text{for } \omega\geqslant\gamma-1. \end{cases} \tag{9}$$

Thus, fluctuations vanish in the large-size limit for $\omega\geqslant\gamma-1$, while for $\omega<\gamma-1$ the fluctuations of $g$ diverge as a power law with the network size $N$.

In the rest of the paper, we will mainly discuss the simplest case $\omega\geqslant\gamma-1$, considering often the cases $\omega=2$ and $\omega=\gamma-1$. The more delicate issue of the effect of outliers on the behavior of the CP on SF networks will be touched on only in Sec. IX. Notice that the value $\omega=2$ has no special meaning here and is just an example of what occurs for $\omega>\gamma-1$. At odds with the case of quenched networks, the structural cutoff $k_c=N^{1/2}$ does not play any role in annealed networks.

## III. THE CONTACT PROCESS ON COMPLEX NETWORKS

We consider the contact process [22] on heterogeneous networks, which is defined as follows [19]. An initial fraction $\rho_0$ of vertices is randomly chosen and occupied by a particle. The dynamics evolves in continuous time by the following stochastic processes. Particles in vertices of degree $k$ create offspring in their nearest neighbors at rate $\lambda/k$, independently of the degree $k'$ of the nearest neighbors. At the same time, particles disappear at a rate $\mu$ that, without loss of generality, is set to $\mu=1$. From a computational point of view, the CP can be efficiently implemented by means of a sequential updating algorithm [19,22]. At each time step $t$, a particle in a vertex $i$ is chosen at random. With probability $p=1/(\lambda+1)$ the particle disappears. On the other hand, with probability $1-p=\lambda/(\lambda+1)$, the particle may generate an offspring. In this case, a vertex $j$, nearest neighbor of $i$, is selected at random. If $j$ is empty, a new particle is created on it; otherwise, nothing happens. In any case, time is updated as $t\to t+[(1+\lambda)n(t)]^{-1}$, where $n(t)$ is the number of particles at the beginning of the time step. Notice that the factor $(1+\lambda)$ in the time update is due to the fact that each infected particle can perform two independent actions, either infect a neighbor (at rate $\lambda$) or become healthy again (at rate $\mu=1$) and, as a consequence, the average interevent time is precisely $[(1+\lambda)n(t)]^{-1}$. This factor was neglected in previous implementations of the CP in complex networks [19,24,25]. The results of these works remain, however, unaltered, since the factor is irrelevant for steady state properties and amounts only to a rescaling for time-dependent properties.

In Euclidean $d$-dimensional lattices, the CP undergoes a nonequilibrium phase transition [22] between an absorbing state, with zero particle density, and an active phase, with average constant density of particles, which takes place at a critical point $\lambda_c$. This phase transition is characterized in terms of the order parameter $\rho$, defined as the average density of particles in the steady state. Defining throughout the paper

$$\Delta = \lambda - \lambda_c, \tag{10}$$

we observe for $\Delta<0$, and in infinite lattices, an absorbing phase with $\rho=0$. For $\Delta>0$, on the other hand, the system stays in an active phase with a nonzero order parameter, obeying $\rho\sim\Delta^{\beta}$. Close to the critical point, the system is also characterized by diverging correlation length and time scales, namely, $\xi\sim|\Delta|^{-\nu_\perp}$ and $\tau\sim|\Delta|^{-\nu_\parallel}$. The critical exponents $\beta$, $\nu_\perp$, and $\nu_\parallel$ characterize the steady state properties of the transition. It is also possible to look at the time-dependent behavior at the critical point. Thus, for example, the particle density is observed to decay in time as $\rho(t)\sim t^{-\theta}$. Different quantities can also be defined to evaluate the time properties of spreading experiments, in which the dynamics evolves starting from a single particle. In this case we can define the survival probability $S(t)$ as the probability that the activity lasts longer than $t$, finding at the critical point $S(t)\sim t^{-\delta}$. These and other critical exponents are not independent, but are related by a set of scaling and hyperscaling relations [22]. Thus it is possible to give a full characterization of the phase transition of the CP in Euclidean lattices using only three exponents, which we can take to be (without lack of generality) $\beta$, $\nu_\perp$, and $\nu_\parallel$. Below the critical dimension $d_c=4$, the exponents are nontrivial, and depend explicitly on $d$. For $d>d_c$, the exponents take the classical MF values $\beta=\nu_\parallel=1$, $\nu_\perp=1/2$.

## IV. HETEROGENEOUS MEAN-FIELD THEORY FOR THE CP

Heterogeneous mean-field theory is the basic starting point to obtain an analytical understanding of the behavior of any dynamical process on a complex network [1]. In order to take into account the possible fluctuations induced by the network connectivity, the partial densities $\rho_k(t)$ of occupied vertices of degree $k$ [8,42] are considered, from which the total density of particles is obtained as $\rho(t)=\Sigma_k\rho_k(t)P(k)$. In the spirit of standard mean-field theories [43], the fact that the quantities $\rho_k(t)$ are, in finite networks, of stochastic nature is neglected. Instead, deterministic rate equations are considered, taking into account the changes in time of the partial densities, due to the different steps that the evolution of the model can take.

In the case of the CP, the quantities $\rho_k(t)$, given by

$$\rho_k(t) = \frac{n_k(t)}{NP(k)}, \tag{11}$$

where $n_k(t)$ is the number of particles on vertices of degree $k$, can be interpreted equivalently as the relative densities of particles on vertices of degree $k$, or the probabilities that a given vertex of degree $k$ contains a particle. In a step of the CP dynamical evolution, the partial density $\rho_k(t)$ can decrease due to the annihilation of a particle in a vertex $k$ (with rate 1), or can increase by the generation of an offspring in a vertex $k'$, nearest neighbor of $k$ (with rate $\lambda/k'$). Therefore, the rate equations for the partial densities in a network characterized by a degree distribution $P(k)$ and degree correlations given by the conditional probability $P(k'|k)$ can be written as [19]

$$\frac{\partial\rho_k(t)}{\partial t} = -\rho_k(t) + \lambda k[1-\rho_k(t)]\sum_{k'}\frac{P(k'|k)\rho_{k'}(t)}{k'}. \tag{12}$$

Given Eq. (12), $\rho_k=0$ is always a solution. The conditions for the presence of nonzero steady states can be obtained by performing a linear stability analysis [44]. Neglecting higher-order terms, Eq. (12) becomes

$$\frac{\partial\rho_k(t)}{\partial t} \simeq \sum_{k'} L_{kk'}\rho_{k'}(t) \equiv \sum_{k'}\left(-\delta_{k,k'} + \lambda k\frac{P(k'|k)}{k'}\right)\rho_{k'}(t). \tag{13}$$

It is easy to see that the Jacobian matrix $L_{kk'}$ has a unique eigenvector $v_k=k$ and a unique eigenvalue $\Lambda=\lambda-1$. Therefore, a nonzero steady state is possible only for $\Lambda>0$, which translates in a critical threshold for the absorbing state phase transition,

$$\lambda_c = 1, \tag{14}$$

independent of the degree distribution and the correlation pattern.

To get more detailed information on the process, and in particular on the shape of the order parameter as a function of the rate $\lambda$, we restrict our attention to uncorrelated networks.

In this case, Eq. (12) reads

$$\frac{\partial \rho_k(t)}{\partial t} = -\rho_k(t) + \lambda \frac{k}{\langle k \rangle}[1-\rho_k(t)]\rho(t). \tag{15}$$

Imposition of the steady state condition $\partial_t \rho_k(t)=0$ yields the nonzero solutions

$$\rho_k = \frac{\lambda k \rho / \langle k \rangle}{1+\lambda k \rho / \langle k \rangle}, \tag{16}$$

where $\rho_k$ is now independent of time. By combining Eq. (16) with the definition of $\rho$, one obtains the self-consistent equation for the order parameter $\rho$,

$$\rho = \frac{\lambda \rho}{\langle k \rangle} \sum_k \frac{kP(k)}{1+\lambda k \rho / \langle k \rangle}, \tag{17}$$

which depends on the full degree distribution.

In the case of SF networks, for which the degree distribution in the continuous degree approximation is given by $P(k)=(\gamma-1)m^{\gamma-1}k^{-\gamma}$, with $m$ the minimum degree in the network, the solution will depend on the degree exponent $\gamma$. Substituting the summation by an integral in Eq. (17), we obtain in the *infinite network size limit* (i.e., when the degree belongs to the range $[m,\infty]$) the expression

$$\rho = F\left[1, \gamma-1, \gamma, -\frac{\langle k \rangle}{\lambda \rho m}\right], \tag{18}$$

where $F[a,b,c,z]$ is the Gauss hypergeometric function [41]. To evaluate the critical behavior for small $\rho$, we invert this expression using the asymptotic expansion of the hypergeometric function for low densities [41], obtaining the result $\rho(\lambda) \sim (\lambda-1)^{\beta}$, with $\beta=1/(\gamma-2)$ for $2<\gamma<3$ and $\beta=1$ for $\gamma>3$, presenting additional logarithmic corrections at $\gamma=3$.

Right at the critical point, $\lambda=1$, the particle density is expected to decay as a power law of time, $\rho(t) \sim t^{-\theta}$ [22], defining a new, temporal, critical exponent. This exponent can be estimated within the HMF method, by considering the time evolution of the total density at $\lambda=1$, namely,

$$\frac{\partial \rho(t)}{\partial t} = \sum_k P(k) \frac{\partial \rho_k(t)}{\partial t} = -\frac{\rho(t)}{\langle k \rangle} \sum_k k \rho_k(t). \tag{19}$$

To close this equation, we use a quasistatic approximation [17], which can be justified in terms of an adiabatic approximation for the full Langevin theory for the CP (see Sec. VI B). In essence, we consider that, even at the critical point, where no steady state is present, the partial densities relax to a quasistationary state, where they take the form given by Eq. (16). In this case, for SF networks in the continuous degree approximation, Eq. (19) will read

$$\frac{\partial \rho(t)}{\partial t} \simeq -\rho(t) F\left[1, \gamma-2, \gamma-1, -\frac{\langle k \rangle}{\rho(t) m}\right]. \tag{20}$$

Using the asymptotic approximation for the hypergeometric function, valid for low density, we obtain a decay exponent in infinite networks given by $\rho(t) \sim t^{-\theta}$, with $\theta=\beta$ for all $\gamma$ (logarithmic corrections being again present at $\gamma=3$).

## V. FINITE-SIZE SCALING FOR THE CP IN COMPLEX NETWORKS

The exponents obtained within HMF theory in the previous section correspond to the thermodynamic limit of a SF network of infinite size. Checking their accuracy in numerical simulations becomes thus a nontrivial task, particularly close to the critical point, due to the effects of finite network sizes. Indeed, because of the small-world property, the number of neighbors that can be reached starting from a certain node grows exponentially or faster with the geodesic distance. This implies that, even for large networks, just a few steps are sufficient to probe the finiteness of the system. Moreover, in SF networks, local topological properties show very strong fluctuations, increasing with the size of the network.

For general critical phenomena, the theory of finite-size scaling (FSS) [45] has successfully overcome this problem for processes taking place on regular lattices, allowing the detection of the signature of continuous phase transitions even in very small systems. For absorbing state phase transitions, FSS is based on the observation that, even below the critical point, the density of active sites (i.e., vertices with a particle on them) in surviving runs $\rho_s$ reaches a quasi-steady-state whose average is a decreasing function of the system size, and which can be expressed as a homogeneous scaling function of both the system size and the distance to the critical point. In the case of networks, system size is replaced by the number of vertices, and the surviving density is assumed to satisfy the relation [46,47]

$$\rho_s(\Delta, N) = N^{-\beta/\bar{\nu}} f(\Delta N^{1/\bar{\nu}}), \tag{21}$$

where $f(x)$ is a scaling function that behaves as $f(x) \sim x^{\beta}$ for $x \to \infty$ and $f(x) \sim$ const for $x \to 0$.

Mean-field theory for homogeneous networks predicts the exponents $\beta=1$ and $\bar{\nu}=2$. For the case of SF networks, Ref. [20] proposed a phenomenological Langevin equation for the particle density, taking the form

$$\frac{d\rho(t)}{dt} = \Delta \rho(t) - b\rho(t)^2 - d\rho(t)^{\gamma-1} + \sqrt{\rho(t)}\,\eta(t), \tag{22}$$

where $\eta(t)$ is an uncorrelated Gaussian noise. Assuming a scaling form for the surviving density given by Eq. (21), and by means of a droplet-excitation argument, the authors of [20] found that $\beta=1/(\gamma-2)$ and $\bar{\nu}=(\gamma-1)/(\gamma-2)$ for $\gamma<3$, independent of the network cutoff, whenever $k_c(N) > N^{1/\gamma}$ [23].

In Ref. [25], this issue was pursued by focusing on the FSS form of survival probability, which at the critical point, and in networks of size $N$, was assumed to be

$$S(t,N) = t^{-\delta} f(t/t_c(N)). \tag{23}$$

The scaling function $f(x)$ is constant for small values of the argument and cutoff exponentially for $x \gg 1$. $t_c(N)$ is a characteristic cutoff time that, according to standard mean-field FSS theory, should scale as $t_c(N) \sim N^{1/2}$ for homogeneous networks [22]. By means of a mapping to a biased, one-dimensional random walk, the authors of [25] found $\delta = 1$, while the characteristic time showed the form, for heterogeneous networks, $t_c(N) \sim \sqrt{N/g}$, where $g$ is defined in Eq. (7), and is thus dependent on the degree cutoff. This surprising result, well confirmed by numerical simulations [25], is in strong disagreement with results of Refs. [20,23], in which no cutoff dependence was claimed.

In order to fully ascertain the correct FSS behavior of the CP in SF networks, we go beyond mean-field and phenomenological theories and tackle the full problem, taking into account its implicit stochastic fluctuations (particularly important in the vicinity of a critical point) by means of a Langevin approach. This problem is considered in the next section.

## VI. LANGEVIN APPROACH FOR THE CP ON NETWORKS

### A. Generic formalism

To account for the stochastic fluctuations of the CP close to the critical point, we derive here a Langevin equation describing the concentration $\rho_k(t)$ or, alternatively, the number of active sites of degree $k$, $n_k(t)$. Our derivation follows closely the method developed in [17]. We start by deriving exact equations for the microscopic dynamics (at the vertex level) of the process. Let $\sigma_i(t)$ be a random binary variable taking value $\sigma_i(t) = 1$ if node $i$ is occupied by a particle at time $t$ and $\sigma_i(t) = 0$ otherwise. Thus, the state of the process at time $t$ is completely determined by the state vector $\boldsymbol{\Sigma}(t) = \{\sigma_1(t), \sigma_2(t), \ldots, \sigma_N(t)\}$. Variables $\sigma_i(t)$ can undergo only two types of transition events.

(1) $\sigma_i(t) = 1 \to \sigma_i(t+dt) = 0$: Vertex $i$ was occupied by a particle at time $t$, and the particle annihilated during the time interval $[t, t+dt]$.

(2) $\sigma_i(t) = 0 \to \sigma_i(t+dt) = 1$: Vertex $i$ was empty at time $t$ and it received an offspring from an occupied nearest neighbor during the time interval $[t, t+dt]$.

Assuming that the temporal occurrence of these events follows Poisson processes, the previous two events can be encoded into a single dynamical equation that describes the evolution of $\sigma_i(t)$ after an increment of time $dt$ as

$$\sigma_i(t+dt) = \sigma_i(t)\zeta_i(dt) + [1 - \sigma_i(t)]\eta_i(dt), \tag{24}$$

where $\zeta_i(dt)$ and $\eta_i(dt)$ are dichotomous random variables taking values

$$\zeta_i(dt) = \begin{cases} 0 & \text{with probability } dt, \\ 1 & \text{with probability } 1 - dt, \end{cases} \tag{25}$$

and

$$\eta_i(dt) = \begin{cases} 1 & \text{with probability } \lambda\, dt \sum_j a_{ij}\sigma_j(t)\dfrac{1}{k_j}, \\ 0 & \text{with probability } 1 - \lambda\, dt \sum_j a_{ij}\sigma_j(t)\dfrac{1}{k_j}. \end{cases} \tag{26}$$

The first term in the right-hand side in Eq. (24) describes the annihilation of one particle at vertex $i$, while the second term describes the creation of one particle in the same (initially empty) vertex. Notice that this is true because each term in this equation depends on two mutually exclusive events: either there is a particle at time $t$, so that $\sigma_i = 1$ and the second term is identically zero, or the site is empty, so that $\sigma_i = 0$ and, thus, the first term is zero.

The set of random variables $\{\zeta_i(dt); i = 1, \ldots, N\}$ are statistically independent of each other and of the conjugate random variables $\{\eta_i(dt); i = 1, \ldots, N\}$. On the other hand, the variables $\{\eta_i(dt); i = 1, \ldots, N\}$ are not totally independent since they may involve common events inducing correlations among them. For example, imagine two empty vertices $A$ and $B$, each of degree 1, connected to the same occupied vertex $C$. Because of the CP dynamics, during a particle reproduction event at vertex $C$, the particle must choose only one of its neighbors to which to send the offspring. Therefore, if vertex $A$ gets the offspring, vertex $B$ cannot receive it, and vice versa, inducing thus correlations between the random variables $\eta_A(dt)$ and $\eta_B(dt)$. However, it is easy to see that these correlations are of order $dt^2$ and can then be safely neglected. In any case, this effect exists only in networks with a quenched topology. In contrast, the annealed network topology changes faster than the CP dynamics and, therefore, such correlations are absent.

Equations (24)–(26) describe the evolution of the state of the system at the most detailed possible level of description by specifying the precise state of each and every one of the vertices of the network. This description, although exact, is not very useful for deriving general properties of the system, which are better described by coarse-grained quantities. In heterogeneous random networks with given degree distribution $P(k)$ and degree-degree correlations $P(k'|k)$, the degree of vertices $k$ is the most appropriate indicator of the different classes of vertices. Therefore, we consider all vertices with the same degree to be statistically equivalent. Following these ideas, let $n_k(t)$ be the number of active vertices of degree $k$ at time $t$, that is,

$$n_k(t) \equiv \sum_{i \in k} \sigma_i(t). \tag{27}$$

As we can see, $n_k(t)$ is the sum of a large number of random variables that are nearly statistically independent in the quenched version of the network and totally independent in its annealed version. Therefore, by invoking the central limit theorem, we expect this variable to follow a Gaussian distribution and, consequently, to follow a Langevin dynamics. To derive the specific form of this Langevin equation, we need to calculate the infinitesimal moments of $n_k(t)$, which can be done using Eqs. (24)–(26). Using the results in Appendix A,

we can finally write the corresponding Langevin equation for the CP on annealed networks, namely,

$$\frac{dn_k(t)}{dt} = -n_k(t) + \lambda[1-\rho_k(t)]\sum_{k'} P(k|k')n_{k'}(t) + \xi_k(t)\sqrt{n_k(t) + \lambda[1-\rho_k(t)]\sum_{k'} P(k|k')n_{k'}(t)}, \tag{28}$$

where $\rho_k(t)=n_k(t)/P(k)N$ is the relative density of active vertices of degree $k$ and $\{\xi_k(t),k=1,\ldots,k_c\}$ are uncorrelated Gaussian white noises (with zero mean and unit variance).

Equation (28) implicitly assumes that $n_k(t)$ is a continuous variable. This approximation is reasonable as long as $n_k(t) \gg 1$, which is usually the case in very large systems, when we consider steady state properties.

Equation (28) is one of the main results of this paper and is also the starting point for our subsequent analysis. As one immediately recognizes, the drift term in Eq. (28) corresponds to the standard mean-field approximation derived in Eq. (12). It is easy to see that the potential associated with this drift term has a stable minimum whenever $\lambda > \lambda_c = 1$, which does not depend on the particular correlation pattern given by $P(k|k')$. The position of this minimum corresponds to the steady solution in the active phase in the thermodynamic limit. The diffusion term, on the other hand, points to a process with multiplicative noise which, as we shall see, has important implications when the system is close to its critical point in finite-size systems.

### B. Uncorrelated random networks

Finding solutions of Eq. (28) for networks with general degree-degree correlations is a rather difficult task. In this paper, we focus on the simplest (but instructive) case of uncorrelated random networks with a given degree distribution $P(k)$. For this class of networks, the transition probability takes the simple form $P(k|k')=kP(k)/\langle k\rangle$, which allows us to write Eq. (28) as

$$\frac{d\rho_k(t)}{dt} = -\rho_k(t) + \lambda\frac{k}{\langle k\rangle}[1-\rho_k(t)]\rho(t) + \sqrt{\frac{1}{N_k}\left(\rho_k(t) + \lambda\frac{k}{\langle k\rangle}[1-\rho_k(t)]\rho(t)\right)}\xi_k(t), \tag{29}$$

where $\rho(t)=\Sigma_k n_k(t)/N=\Sigma_k P(k)\rho_k(t)$ is the global concentration of active nodes at time $t$ and we have divided Eq. (28) by the number of vertices of degree $k$, $N_k=NP(k)$. Analogously, we can write a Langevin equation for $\rho(t)$ as

$$\frac{d\rho(t)}{dt} = \rho(t)\left(\Delta - \lambda\sum_k \frac{kP(k)}{\langle k\rangle}\rho_k(t)\right) + \sum_k P(k)\sqrt{\frac{1}{N_k}\left(\rho_k(t) + \lambda\frac{k}{\langle k\rangle}[1-\rho_k(t)]\rho(t)\right)}\xi_k(t), \tag{30}$$

where we have defined $\Delta \equiv \lambda - 1$ so that the critical point corresponds to $\Delta = 0$.

Equation (30) is not yet a closed equation for $\rho(t)$ because both the drift and diffusion terms involve the partial densities $\rho_k(t)$. To close it, we use an adiabatic approximation [48]. From Eq. (30) we know that close to the critical point $\Delta \approx 0$, $\rho(t)$ is a slowly varying variable. This is due to the fact that the first term in the right-hand side of Eq. (30) is of order higher than $\rho$. On the other hand, $\rho_k(t)$ is a variable that relaxes exponentially fast to its quasiequilibrium state since the lowest order in Eq. (29) is linear in $\rho_k$.[3] The adiabatic approximation consists in neglecting the term $d\rho_k(t)/dt$ in front of $\rho_k(t)$ and assuming that $\rho_k$ is a stochastic variable that evolves much faster than $\rho(t)$. Thus, setting $d\rho_k(t)/dt = 0$ in Eq. (29) and solving for $\rho_k(t)$, we obtain

$$\rho_k(t) \approx \frac{\lambda k\rho(t)}{\langle k\rangle + \lambda k\rho(t)} + \frac{\langle k\rangle}{\langle k\rangle + \lambda k\rho(t)}\sqrt{\frac{1}{N_k}\left(\rho_k(t) + \lambda\frac{k}{\langle k\rangle}[1-\rho_k(t)]\rho(t)\right)}\xi_k(t). \tag{31}$$

The noise term in this equation is subdominant due to its dependence on the size of the system. Thus, replacing the dominant term in the diffusion one, we finally obtain

$$\rho_k(t) \approx \frac{\lambda k\rho(t)}{\langle k\rangle + \lambda k\rho(t)} + \sqrt{\frac{1}{N_k}\frac{2\lambda k\rho(t)\langle k\rangle^2}{[\langle k\rangle + \lambda k\rho(t)]^3}}\xi_k(t). \tag{32}$$

In this way, we obtain an expression for the partial densities $\rho_k$ as a function of $k$ and $\rho(t)$ only. Replacing this expression in Eq. (30) and keeping only the first order in $N_k^{-1}$, we obtain

$$\frac{d\rho(t)}{dt} = \rho(t)\left(\Delta - \lambda\sum_k \frac{kP(k)}{\langle k\rangle}\frac{\lambda k\rho(t)}{\langle k\rangle + \lambda k\rho(t)}\right) + \sum_k P(k)\sqrt{\frac{1}{N_k}\frac{2\lambda k\rho(t)\langle k\rangle^2}{[\langle k\rangle + \lambda k\rho(t)]^3}}\xi_k(t). \tag{33}$$

Notice that the sum of statistically independent Gaussian white noises is another Gaussian white noise whose variance is the sum of the individual variances. Thus, the diffusion term in the last equation is, indeed, a Gaussian white noise. Therefore, we can finally write

$$\frac{d\rho(t)}{dt} = \rho(t)(\Delta - \lambda\Theta[\rho(t)]) + \sqrt{\frac{2\lambda\rho(t)}{N}\Lambda[\rho(t)]}\xi(t), \tag{34}$$

where

$$\Theta[\rho(t)] \equiv \sum_k \frac{kP(k)}{\langle k\rangle}\frac{\lambda k\rho(t)}{\langle k\rangle + \lambda k\rho(t)} \tag{35}$$

and

[3] It is worth mentioning that this separation of time scales between the partial quantities $\rho_k$ and the global one $\rho$ has also been observed in other dynamics, like the $A+A\to\emptyset$ diffusion-annihilation process [17] or the voter models [49].

$$\Lambda[\rho(t)] \equiv \sum_k \frac{kP(k)}{\langle k\rangle} \frac{\langle k\rangle^3}{[\langle k\rangle + \lambda k\rho(t)]^3}. \quad (36)$$

The term $\Theta[\rho]$ can be interpreted as the probability that, following a randomly chosed edge, we arrive at a vertex occupied by a particle. Equation (34) is now a closed equation for the total density of active vertices, $\rho$, which must be solved with an absorbing boundary at $\rho=0$ and a reflecting one at $\rho=1$. As we can see from Eq. (34), there is an explicit dependence on the size of the network, $N$, in the diffusion term of the Langevin equation. This size dependence, together with the specific functional forms of $\Theta[\rho]$ and $\Lambda[\rho]$ will determine the finite-size behavior of the system near the critical point.

## VII. CP IN ANNEALED SCALE-FREE NETWORKS

In this section we focus on heterogeneous networks with a power-law degree distribution $P(k)\sim k^{-\gamma}$ with $k\in[m,M]$, where $2<\gamma<3$, and $M=N^{1/\omega}$ is the degree upper cutoff. In particular, we consider the case $\omega\geqslant\gamma-1$, so that the average maximum of the degree distribution $k_c\sim M=N^{1/\omega}$ is a hard cutoff (Sec. II). The case $\omega<\gamma-1$ will be considered in Sec. IX.

Given the form of the degree distribution it is possible to evaluate explicitly the functional form of $\Theta[\rho]$, which determines the dynamical properties of the CP. From its definition, Eq. (35), it is easy to see that in the limit of small density $\Theta[\rho]$ has two different functional forms depending on whether $\rho$ is larger or smaller than the quantity $\langle k\rangle/\lambda k_c$, $k_c$ being the network cutoff. Thus we have (see Appendix B)

$$\Theta[\rho] = \begin{cases} g\lambda\rho, & \rho \ll \dfrac{\langle k\rangle}{\lambda k_c}, \quad \text{region II}, \\ C(\gamma)\left(\dfrac{\lambda\rho}{\langle k\rangle}\right)^{\gamma-2}, & \dfrac{\langle k\rangle}{\lambda k_c} \ll \rho \ll 1, \quad \text{region I}, \end{cases} \quad (37)$$

where $g=\langle k^2\rangle/\langle k\rangle^2$ and

$$C(\gamma) = m^{\gamma-2}\Gamma(\gamma-1)\Gamma(3-\gamma). \quad (38)$$

We denote the regime for small $\rho$ as region II, and the regime for larger $\rho$ as region I. Analogously, we can evaluate the behavior of the function $\Lambda$ as

$$\Lambda[\rho] = \begin{cases} 1, & \text{region II}, \\ 1-\tilde{C}(\gamma)\left(\dfrac{\lambda\rho}{\langle k\rangle}\right)^{\gamma-2}, & \text{region I}, \end{cases} \quad (39)$$

with

$$\tilde{C}(\gamma) = \tfrac{1}{2}m^{\gamma-2}(\gamma-2)(\gamma-1)\Gamma(1+\gamma)\Gamma(1-\gamma). \quad (40)$$

As we can see, the correction term in region I is always very small as compared to 1. Therefore, in the rest of the paper we consider that $\Lambda[\rho]=1$.

In Fig. 1 the behavior of $\Theta[\rho]$ is evaluated by numerically performing the summation in Eq. (35). The linear behavior for small densities is very well obeyed. Instead, the scaling

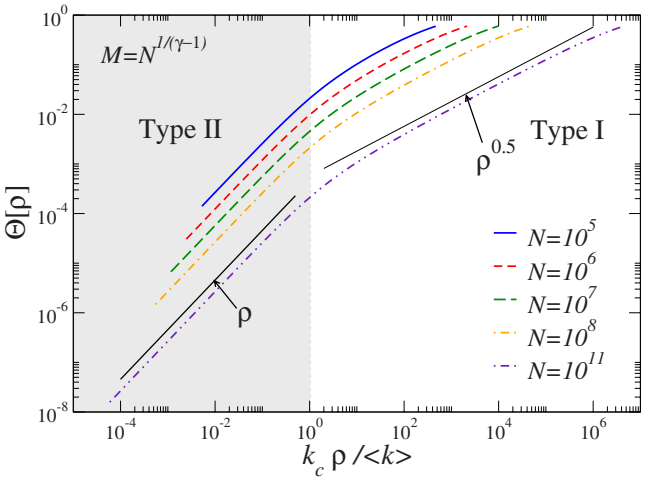


FIG. 1. (Color online) Numerical evaluation of the function $\Theta[\rho]$ as a function of $k_c\rho/\langle k\rangle$ for different network sizes. The degree exponent is $\gamma=2.5$ and we use $\omega=\gamma-1$ and $m=2$. In the type II region, it is clearly visible a linear behavior, in agreement with Eq. (37). In the type I region, convergence toward the theoretical expression given by Eq. (37) is much slower. We need to reach sizes of the order $N=10^{11}$ to clearly see the thermodynamic limit behavior $\rho^{1/2}$. Black solid lines are guides to the eye for the two expected behaviors $\rho$ and $\rho^{1/2}$.

of the region I is not cleanly observed even for the largest network considered ($N=10^8$). This is due to the fact that region I is surrounded by two slow crossovers, one for $\rho\approx\langle k\rangle/k_c$ (where the transition between region I and II takes place) and the other for $\rho=1$ (where $\Theta$ becomes independent of $\rho$). This has the consequence that some of the theoretical predictions made using the simple approximation given in Eq. (37) are difficult to observe except for extremely large system sizes.

As a consequence of the form of $\Theta[\rho]$, the behavior of the system at criticality strongly depends on the type of numerical experiment performed to probe the absorbing transition (see Fig. 2). Indeed, experiments with stochastic trajectories exploring the region $\rho\gg\langle k\rangle/\lambda k_c$ experience a drift of the form

$$\Psi[\rho] \simeq \rho\left(\Delta - C(\gamma)\left(\frac{\lambda\rho}{\langle k\rangle}\right)^{\gamma-2}\right) \quad \text{(type I drift)}. \quad (41)$$

Instead, any experiment such that trajectories mainly stay in the region $\rho\ll\langle k\rangle/\lambda k_c$ experiences a drift term of the form

$$\Psi[\rho] = \rho(\Delta - \lambda^2 g\rho) \quad \text{(type II drift)}. \quad (42)$$

The quantity $g$, which will play a fundamental role in the rest of the paper, diverges with the cutoff $k_c$ as $k_c^{\gamma-3}$ for $\gamma<3$ (and $\omega>\gamma-1$). Notice that for $\gamma>3$ the leading order is linear in both cases. It is also worth stressing that, if one lets $k_c$ diverge, regime II disappears and one is left only with regime I, which coincides with what is found using HMF theory on infinite networks (Sec. IV). However, in any finite network, when the density gets small it is the drift of type II that rules the dynamics.

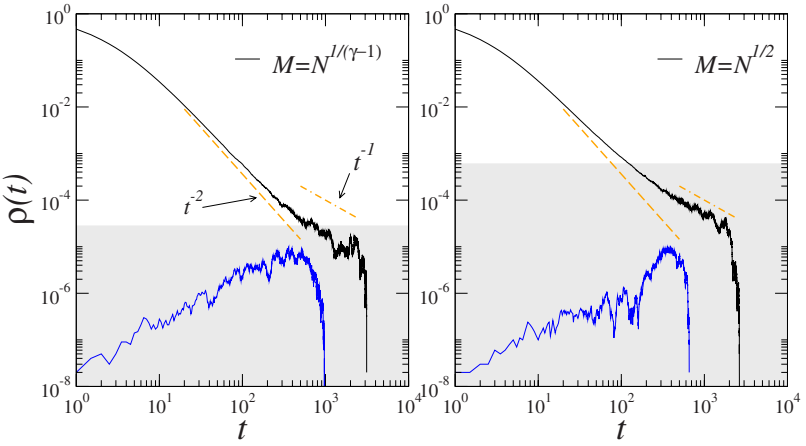


FIG. 2. (Color online) Example of two different types of numerical experiment (i.e., Monte Carlo simulations) to study the CP dynamics at criticality performed in an annealed network of size $N=10^8$, $\gamma=2.5$, and $m=2$. The top (black) curve is the density decay starting from a fully active network. The bottom (blue) curve corresponds to a spreading experiment starting from a single active vertex. The left plot corresponds to the hard cutoff $M=N^{1/(\gamma-1)}$ and the right plot to $M=N^{1/2}$. Gray areas depict the values of $\rho$ in the domain $\rho \in [N^{-1}, \langle k \rangle k_c^{-1}]$. In all cases trajectories are for a single run in a single network realization.

Based on the explicit expression of $\Theta[\rho]$ we now provide a qualitative and quantitative description of the three types of experiment that explore the critical properties of the CP dynamics: (A) density decay at criticality, (B) spreading experiments, and (C) surviving runs.

### A. Density decay at criticality

Starting from a configuration full of active vertices at $t=0$, the concentration of active vertices is monitored as a function of time until it reaches the absorbing state $\rho=0$. Then an average is performed over a large number of different runs up to a time such that all runs have survived. In this case, after a initial time scale $t_\times$, the system first experiences the type I drift and after a crossover time $t^*$, at very low concentrations, the type II one. Inserting Eq. (41) into Eq. (34), a pure drift of the type I predicts a behavior $\rho_{\mathrm{I}}(t) \sim t^{-\theta}$ with $\theta=1/(\gamma-2)$. Inserting Eq. (42) gives instead $\rho_{\mathrm{II}}(t) \sim (gt)^{-1}$. The crossover between the two types of behavior occurs for a time $t^*$ such that $\rho_{\mathrm{II}}(t^*) \simeq \langle k \rangle / k_c$, i.e., $t^* \sim k_c/(g\langle k \rangle) \sim \langle k \rangle k_c^{\gamma-2}$. A third time scale defines the survival time of the different runs that, as we will see in the next subsection, scales as $t_c \sim \sqrt{N/g}$.

Figure 2 shows simulation results for this type of experiment (top curves) in annealed networks with $\gamma=2.5$, $m=2$, for $\omega=2$ or $\omega=\gamma-1$ for a single run starting from a fully active network. Different colors (gray and white) indicate the different regions depending on the shape of the drift term. The first thing to notice is that, in the case of $\omega=\gamma-1$, the region that corresponds to the type I drift is wider as compared to the case $\omega=2$. Nevertheless, even in this optimal case, we do not observe cleanly the two different values of the exponent $\theta$. For comparison purposes, in Fig. 2 we also plot functions $t^{-2}$ and $t^{-1}$ that would correspond to the pure type I and II behaviors for $\gamma=2.5$. The exponent $\theta$ approaches but does not reach the theoretical value $\theta=2$ even though simulations are performed in networks of size $N=10^8$. The situation in the case of $\omega=2$ is even worse because the crossover happens at shorter times and the value $\theta=2$ is even more difficult to observe.

The same is observed in Fig. 3, where we show the same as Fig. 2 for networks with $\gamma=2.5$, $\omega=2$, and different network sizes but averaging over 100 runs of the process over the same network realization. Additional information is provided by the local effective exponent of the temporal decay as a function of time (Fig. 4). The effective exponent decreases initially quite fast, but even for $N=10^8$ the crossover to regime II takes place well before the asymptotic value $\theta=1/(\gamma-2)=2$ is reached. Eventually the effective exponent reaches a constant value, which is, quite surprisingly, close to 1.2 instead of the expected value $\theta=1$.

The reason why we do not see convincing numerical evidence of either of the two scaling exponents expected from the theory is that the separation of time scales between $t_\times$, $t^*$, and $t_c$ is too weak. To observe cleanly the two different regimes the time scales must be well separated, $t_\times \ll t^* \ll t_c$, and this requires very large values of $N$. Two additional elements make the observation of the expected scaling of type I, $\theta=1/(\gamma-2)$, even more difficult. First, the time for the onset of scaling (see Appendix C),

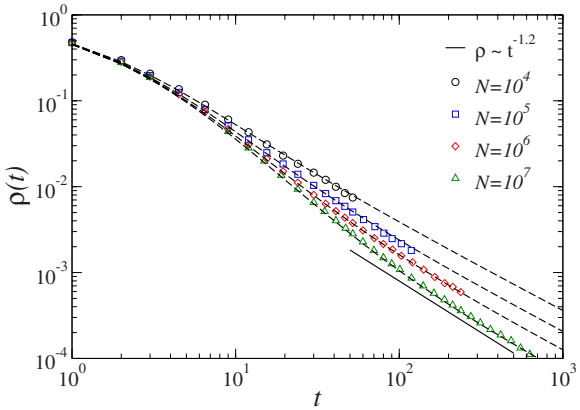


FIG. 3. (Color online) Evolution of the concentration $\rho(t)$ starting from a fully infected network for different network sizes, $\gamma=2.5$, $m=2$, and $\omega=2$. Results are averaged over 100 realizations in a single network realization. Long-dashed lines correspond to the numerical solution of the set of Eqs. (15), using as input the empirical degree sequence used in the simulations. The very nice agreement between both sets of curves justifies our approximation. The solid line decaying as $t^{-1.2}$ is a guide to the eye.

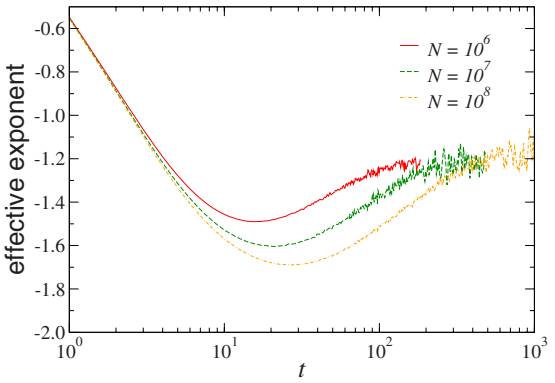


FIG. 4. (Color online) Local effective exponent as a function of time for $\gamma=2.5$, $\omega=2$, $m=2$, and various values of $N$. The exponent corresponding to the discrete time $t_i$ is given by the slope of the line joining $\rho(t_{i-1})$ and $\rho(t_{i+1})$ in log-log scale.

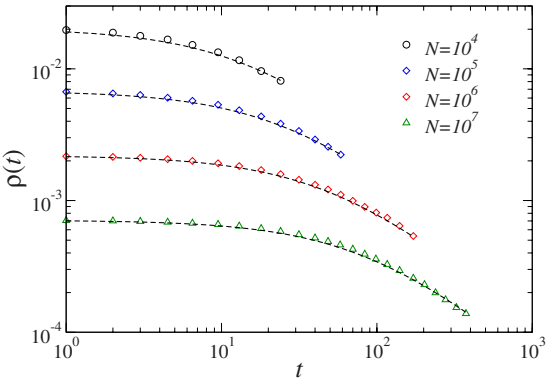


FIG. 5. (Color online) Evolution of the concentration $\rho(t)$ in region II for different network sizes, $\gamma=2.5$, $m=2$, and $\omega=2$. The initial concentration is $\rho_0=\langle k\rangle/2k_c$ and results are averaged over 500 realizations. Dashed lines correspond to the theoretical prediction Eq. (44).

$$t_\times = \frac{\rho_0^{2-\gamma}(\gamma-1)^{\gamma-2}}{(\gamma-2)^{\gamma-1}\Gamma(3-\gamma)\Gamma(\gamma-1)}, \tag{43}$$

can be quite large and it diverges for $\gamma\to 2$. Second, the convergence of $\Theta[\rho]$ to its asymptotic shape is very slow (Fig. 1). Despite these difficulties, Fig. 4 suggests that by increasing the size of the system we should eventually be able to recover the theoretical exponent $\theta=1/(\gamma-2)$.

Concerning the exponent corresponding to the type II drift, $\theta=1$, its evaluation from Fig. 4 is more difficult. For instance, in the case $\omega=\gamma-1$ the scaling of $t^*$ and $t_c$ is the same and, therefore, the exponent $\theta=1$ can barely be observed. In the case $\omega=2$, they scale as $t^*\sim N^{(\gamma-2)/2}$ and $t_c \sim N^{(\gamma-1)/4}$. Their ratio then goes as $t^*/t_c\sim N^{(\gamma-3)/4}$ (1/8 for $\gamma=2.5$) which is a very small exponent. The direct consequence is that the evaluation of the exponent $\theta=1$ from this type of experiment is too much influenced by the effect of the crossover between regions I and II.

To clearly see the predicted behavior corresponding to the type II drift, we perform numerical simulations with an initial concentration $\rho_0$ well below the critical level separating regions I and II. In particular we choose $\rho_0=\langle k\rangle/2k_c$. With this initial condition the dynamics is ruled by the type II drift from the very beginning, leading to the prediction

$$\rho_{II}(t) = \frac{1}{gt+\rho_0^{-1}}. \tag{44}$$

In Fig. 5, we show simulation results for different network sizes as compared to the prediction given by Eq. (44). The agreement is very good if we consider that the dashed lines in Fig. 5 are generated without fitting any parameter but using the values of $g$ and $\rho_0$ used in the simulations.

The conclusion is that observation observing in simulations of the exponent $\theta=1/(\gamma-2)$ predicted by the mean-field theory in the thermodynamic limit is, although in principle possible as a preasymptotic regime, too difficult from a practical point of view, since one should reach network sizes that are beyond the capabilities of current computers. From Fig. 4, by extrapolating the height of the minimum for the different curves, one can estimate that in order to reach an effective exponent close to 2 a network larger than $N \approx 10^{11}$ should be considered. On the other hand, the behavior predicted by type II drift spans for a shorter time as compared to the type I but is, nevertheless, clearly visible, as shown in Fig. 5.

### B. Spreading experiments

Starting from a single randomly chosen active vertex, the activity is followed until it decays into the absorbing state and the survival time $t$ is recorded. The survival probability $S(t)$, defined as the probability that activity lasts longer than $t$, behaves at the critical point as given by Eq. (23).

Figure 2 shows examples of single realizations of this experiment (bottom blue curves). In this example, though, we have selected realizations that survived a time longer than $10^3$, which roughly corresponds to the value of the cutoff time $t_c$ for this particular $\gamma$ and $N$. In this way we can see the domain of $\rho$ space that is visited by the trajectories of the experiment. For both $\omega=\gamma-1$ and $\omega=2$, trajectories never reach the white area, where the type I drift is dominant. They always remain in the domain governed by the type II drift.

The result of Eq. (23) can be derived from the Langevin equation (34), using standard techniques of stochastic process theory [48]. In Appendix D, we show that, in the limit of an infinite network size, we have

$$S(t) = \lim_{N\to\infty} S(t,N) = 1 - e^{-1/t} \approx \frac{1}{t}, \tag{45}$$

that is, we recover the exponent $\delta=1$ for any degree exponent $\gamma$.

The value of this exponent implies that the probability density function of survival times in infinite systems follows a power law of the form $\psi(t)\sim t^{-2}$ and, therefore, has diverging fluctuations. However, in finite-size systems, this distribution has a size-dependent cutoff time $t_c(N)$, and the divergence of the second moment of survival times $T_2=\langle t^2\rangle$ is then cutoff by $t_c(N)$: $T_2=2\int tS(t,N)dt\sim 2\int^{t_c} t^{1-\delta}\sim t_c(N)$. A calculation of this second moment (Appendix D) leads to the final result

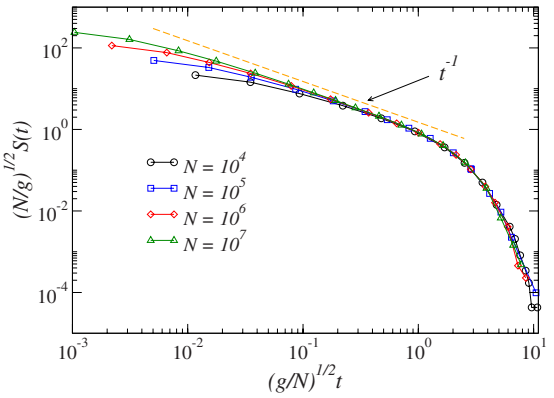


FIG. 6. (Color online) Scaling of the survival probability $S(t)$ for $\gamma=2.5$, $m=2$, and $\omega=\gamma-1$ in a single network realization.

$$t_c(N) \propto \sqrt{\frac{N}{g}}. \tag{46}$$

This expression has an explicit dependence on the size of the system but also an implicit one through the size dependence of the factor $g$ which, as we have shown before, can diverge for $\gamma<3$ with the system size in arbitrary ways. This, indeed, results in an infinite number of ways to approach the thermodynamic limit [25]. For $\gamma>3$ instead, $g$ is a constant and Eq. (46) reproduces the well-known result of homogeneous MF theory [22].

In Ref. [25] it was shown that Eq. (23) is obeyed for $\omega=2$ with the scaling of $t_c(N)$ given by Eq. (46), while it is not if no bound is imposed on the degree distribution. Figure 6 shows that the scaling (23) holds also for $\omega=\gamma-1$ with a hard bound. The violation of the scaling occurring when $\omega<\gamma-1$ is then related not to the average value of the maximum degree $k_c\sim N^{1/(\gamma-1)}$ but to the presence of outliers with exceptionally high values of $k$.

### C. Surviving runs

In this type of experiment, starting from a given initial concentration, only those trajectories that have survived for a fixed observation time $T>t_c$ are kept and used to compute an average concentration of active vertices at criticality $\rho_s$. From a numerical point of view, analogous information can be obtained by means of a surviving average [22], made over the surviving representatives of a large number of independent runs.

The motivation for this type of experiment can be traced back to the FSS theory. According to this phenomenological theory, the concentration of active vertices in surviving runs satisfies the scaling relation [22]

$$\rho_s(\Delta,N) = N^{-\beta/\bar{\nu}} f(\Delta N^{1/\bar{\nu}}). \tag{47}$$

For SF networks with $2<\gamma<3$, the phenomenological approach in Ref. [20] predicted $\beta=1/(\gamma-2)$ and $\bar{\nu}=(\gamma-1)/(\gamma-2)$ (see Sec. V). The values of these exponents are recovered if one considers the type I drift alone. In this section, we show that, in fact, FSS only holds for heterogeneous networks in the case of $\omega=\gamma-1$. Even in this case, because of the slow convergence of the type I drift (e.g., Fig. 1), the FSS theory presented in [20] can be observed only for extremely large systems. This goes against the original idea of FSS, which is used to recover the critical exponents without the need to reach very large systems.

A critical issue in any FSS theory is the computation of the exponent $\beta/\bar{\nu}$. According to Eq. (47), at the critical point we expect that the concentration of active vertices in surviving runs satisfies

$$\rho_s(0,N) \sim N^{-\beta/\bar{\nu}}. \tag{48}$$

In surviving run experiments, one selects only those trajectories that have survived for an arbitrary amount of time. Therefore, the probability density function that there are $n$ active vertices at time $t$ restricted only to surviving runs is

$$p_s(n,t|n_0) = \frac{p(n,t|n_0)}{S(t|n_0)}, \tag{49}$$

where $p(n,t|n_0)$ is the same probability but measured for all trajectories, that is, including those that are absorbed at the boundary. Notice that with this definition $\int dn\, p_s(n,t|n_0)=1$. We are interested in the long-time limit of this probability density function, $p_s(n)=\lim_{t\gg 1} p_s(n,t|n_0)$. In this limit, the concentration of active vertices at criticality for surviving runs is just

$$\rho_s(0,N) = \frac{1}{N}\int np_s(n)dn. \tag{50}$$

The probability density function $p(n,t|n_0)$ satisfies a Fokker-Planck equation, whose solution allows us to compute the surviving density (see Appendix E)

$$\rho_s(0,N) \propto \frac{1}{N}\Bigg[\sqrt{\frac{\pi N}{2g}}\,\mathrm{erf}\left(\sqrt{\frac{\langle k\rangle^2 gN}{2k_c^2}}\right) + \frac{1}{C(\gamma)}\left(\frac{C(\gamma)\langle k\rangle N}{\gamma-1}\right)^{(\gamma-2)/(\gamma-1)} \times\Gamma\left(\frac{1}{\gamma-1},\frac{C(\gamma)\langle k\rangle N}{(\gamma-1)k_c^{\gamma-1}}\right)\Bigg], \tag{51}$$

where $\mathrm{erf}(z)$ and $\Gamma(a,z)$ are the error and incomplete Gamma functions, respectively; the first (second) term in the right-hand side comes from type II (type I) drift. At this point, the result depends on the particular choice of $\omega$. Suppose first that $\omega>\gamma-1$. In this case, both the argument of the error function and that of the incomplete Gamma function diverge as $N\to\infty$. As a consequence, the contribution of the type I potential is exponentially small and only the first integral contributes in the thermodynamic limit, yielding the result

$$\rho_s(0,N) \propto \frac{1}{\sqrt{gN}}. \tag{52}$$

In the case of $\omega=\gamma-1$, the arguments of both the error function and the incomplete Gamma function are constants in the large-size limit. In this case the contribution of both terms is of the same order in $N$, $\rho_s(0,N)\propto N^{-1/(\gamma-1)}$. Nevertheless, since the effective potential $\phi(n,N)$ is a monotonically in-

creasing function of $n$, the contribution in Eq. (51) of the type I potential is always smaller than that of type II. The physical picture is that trajectories stay most of the time in region I except for short excursions to region II, which give a small contribution that, nevertheless, is of the same order in $N$. Therefore, we can conclude that the behavior given by Eq. (52) holds in the whole domain $\omega \in [\gamma-1, 2]$. In terms of $\omega$, we can finally write that

$$\frac{\beta}{\bar{\nu}} = \frac{1}{2} + \frac{3-\gamma}{2\omega}. \tag{53}$$

This result implies that the conclusions drawn in Refs. [20,23] are essentially incorrect, since the scaling of $\rho_s(0,N)$ depends explicitly on the degree cutoff. The exponent ratio $\beta/\bar{\nu}$ obtained in [20,23] is recovered only in the particular case $\omega=\gamma-1$.

## VIII. THE MEANING OF FINITE-SIZE SCALING

With all these results at hand, we can now discuss the role, if any, of FSS theory in the context of absorbing phase transitions in SF networks. The aim of the FSS ansatz is to connect the behavior of the system in the active phase—which is independent of the size of the system—for $\Delta \gg N^{1/\bar{\nu}}$ and the absorbing one—where there is an explicit size dependence—for $\Delta \ll N^{1/\bar{\nu}}$. However, the ability to do so relies upon the "natural" assumption that the laws ruling the system do not change when one performs this transition. In the case of the CP dynamics in SF networks, we have shown that in the absorbing phase the system is mainly ruled by type II drift. However, when $\Delta$ is increased, the concentration of active vertices also increases and eventually the system starts experiencing the type I drift. We are then in a situation where there is a change of the underlying laws between the active and absorbing phases. Consequently, FSS theory does not work in this case. Nevertheless, there are some subtle details depending on the type of cutoff that we discuss next.

In the case of $\omega \geqslant \gamma-1$, the Langevin equation describing the dynamics for the concentration $\rho$ is

$$\frac{d\rho(t)}{dt} = \rho(t)[\Delta - \lambda^2 g \rho(t)] + \sqrt{\frac{2\lambda\rho(t)}{N}}\xi(t) \tag{54}$$

which holds if $\Delta \ll \lambda g\langle k\rangle/k_c$. If we perform the change of variables $N_{ef}=N/g$ and $\rho_{ef}=n/N_{ef}$, the previous equation becomes

$$\frac{d\rho_{ef}(t)}{dt} = \rho_{ef}(t)[\Delta - \lambda^2 \rho_{ef}(t)] + \sqrt{\frac{2\lambda\rho_{ef}(t)}{N_{ef}}}\xi(t). \tag{55}$$

Notice that this equation describes the CP dynamics in a homogeneous network of effective size $N_{ef}$. Therefore, $\rho_{ef}(\Delta, N_{ef})$ must satisfy FFS with exponents $\beta=1$ and $\bar{\nu}=2$, that is,

$$\rho_{ef}(\Delta, N_{ef}) = \frac{1}{\sqrt{N_{ef}}} f(\Delta\sqrt{N_{ef}}). \tag{56}$$

Undoing the change of variables we conclude that $\rho_s(\Delta, N)$ satisfies the anomalous FSS

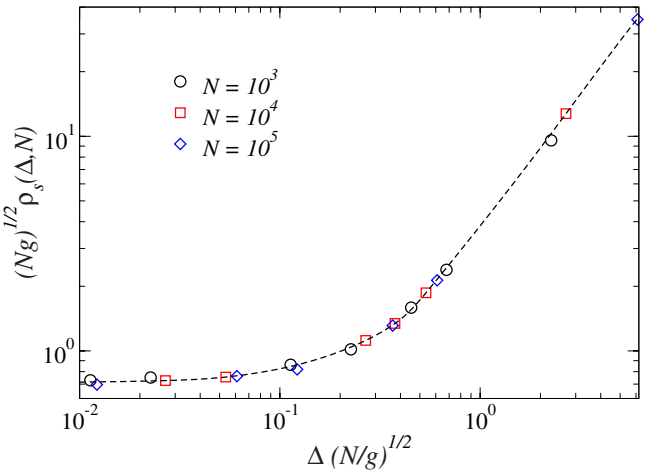


FIG. 7. (Color online) Scaling of the density for surviving runs for $\gamma=2.2$ and $\omega=2$ ($m=2$). Each point is the result of $10^2$ realizations of the stochastic process on each of the $10^2$ network realizations. The dashed line is an interpolation of the data as a guide to the eye.

$$\rho_s(\Delta, N) = \frac{1}{\sqrt{gN}} f\left(\Delta\sqrt{\frac{N}{g}}\right) \quad \text{for } \Delta \ll \frac{\lambda g\langle k\rangle}{k_c}. \tag{57}$$

This FSS is anomalous in the sense that when $\Delta > \sqrt{g/N}$ then $\rho_s(\Delta, N) \sim \Delta/g$, which depends on the size of the system through the factor $g$. Notice also that for $\gamma<3$ the factor $g/k_c$ can be reasonably large even for large system sizes and, consequently, this anomalous scaling can be observed in a wide range of values of $\Delta$. Figure 7 confirms the validity of Eq. (57).

## IX. THE EFFECT OF OUTLIERS

In the previous sections, we have assumed that the maximum allowed degree of the network $M$ scales with the system size $N$ as $N^{1/\omega}$, with $\omega \geqslant \gamma-1$, so that the average cutoff in the degree distribution $k_c$ is proportional to $M$ and degrees much larger than $k_c$ are simply forbidden.

When $M$ scales faster than $N^{1/(\gamma-1)}$ instead, the cutoff degree $k_c$ is not a hard but a soft statistical value: the maximum degree $k_{\max}$ in a single realization of the network is the result of a random process that yields $k_c$ on average but has diverging fluctuations: it is still possible to find outlier vertices having degrees much larger that $k_c$. To investigate the role of outliers in the CP dynamics, we introduce a minimal toy network model with a hard cutoff $k_c \leqslant N^{1/(\gamma-1)}$, just as in the previous sections, and then we add a single vertex of degree $k_{\text{out}}=\alpha N$, with $\alpha \in [0,1]$.

From Eq. (31) we see that the concentration in the outlier vertex is $\rho_{k_{\text{out}}} \approx 1$ provided that $\rho \gg \langle k\rangle/(\lambda\alpha N)$, where the average degree must be computed including the contribution of the outlier. This condition is satisfied in both density decay and surviving run experiments. In the case of spreading experiments, the condition is satisfied only partially since during the beginning of the experiment the density is always of the order $\rho \sim N^{-1}$. However, in the first two types of experiment, the effect of the outlier vertex is that the rest of the

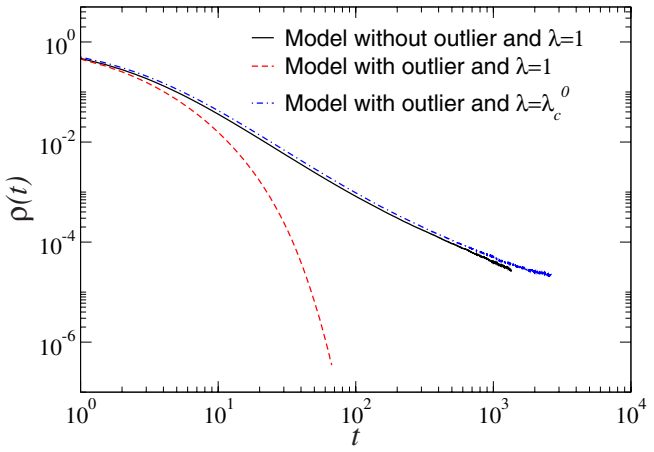


FIG. 8. (Color online) Density decay starting from a fully active network for the model with and without outlier. Network size is $N=10^8$, $m=2$, $\gamma=2.5$, and $M=N^{1/2}$. Results are averaged over 100 realizations in a single instance network.

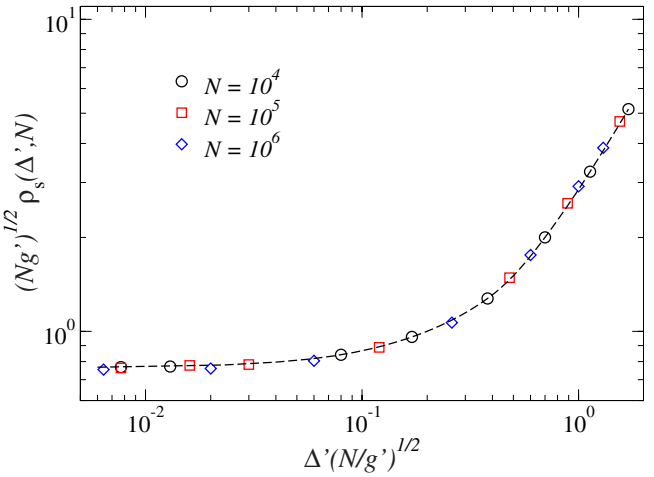


FIG. 9. (Color online) Scaling of the density for surviving runs for $\gamma=2.5$, $m=2$, and $\omega=2$, with outlier of degree $k_{\text{out}}=N$. Each point is the result of $10^4$ realizations of the stochastic process on a single network realization. The dashed line is an interpolation of the data as a guide to the eye.

vertices "see" the outlier as always active. Since the outlier holds a macroscopic portion of the edges of the system, all attempts to make it active occurring along one of its edges are unsuccessful. The net effect is that the system is shifted away from its critical point $\lambda=1$ and is effectively in a subcritical state. To quantify this effect and to calculate the position of the new critical point, we separate in Eq. (35) the outlier's contribution from that of the rest of the vertices. This results in

$$\Theta[\rho(t)] = \sum_{k\neq k_{\text{out}}}^{k_c} \frac{kP(k)}{\langle k\rangle} \frac{\lambda k\rho(t)/\langle k\rangle}{1+\lambda k\rho(t)/\langle k\rangle} + \frac{k_{\text{out}}}{N\langle k\rangle}, \tag{58}$$

that is, the outlier has a constant contribution to the drift term whereas the contribution of the rest of the vertices goes to zero when $\rho$ approaches zero. Combining this result with Eq. (34), we obtain the new critical point

$$\lambda_c^0 = \frac{1}{1-k_{\text{out}}/N\langle k\rangle}. \tag{59}$$

To check this result, we perform numerical simulations starting from a fully active network in three different scenarios (see Fig. 8). In the first one, we generate a network with $M=N^{1/2}$ and set the dynamics to its critical value $\lambda=1$. Here, $\lambda=1$ is the true critical point and, as expected, we find a double power-law decay toward the absorbing state, as explained in Sec. VII. In the second scenario, we introduce in the previous network a single vertex of degree $k_{\text{out}}=N$ and, again, set $\lambda=1$. In this case, we observe a clear exponential decay, typical of a subcritical regime. Finally, in the third experiment, we keep the network with the outlier but we increase the control parameter according to Eq. (59). After this correction to the critical point, we observe again a clear double power-law decay toward the absorbing state, indicating that, indeed, Eq. (59) predicts the correct critical point $\lambda_c^0$.

Along the same lines it is possible to understand also surviving runs in the same network with an outlier. The equation of motion for the density $\rho$ at the new critical point $\lambda=\lambda_c^0$ is

$$\frac{d\rho(t)}{dt} = -(\lambda_c^0)^2 g'\rho^2(t) + \sqrt{\frac{2\rho(t)}{N}}\xi(t), \tag{60}$$

where

$$g' = \sum_{k\neq k_{\text{out}}} k^2 P(k)/\langle k\rangle^2. \tag{61}$$

After redefining time in Eq. (60) as $t'=(\lambda_c^0)^2 t$, we recover the same type of Langevin equation as for the case $\omega\geq\gamma-1$, Eq. (54), but with an effective parameter $g'$ given by Eq. (61). From here, we readily obtain the FSS form for the average density in surviving experiments, namely,

$$\rho_s(\Delta',N) = \frac{1}{\sqrt{g'N}} f\left(\Delta'\sqrt{\frac{N}{g'}}\right), \tag{62}$$

where $\Delta'=\lambda-\lambda_c^0$. In Fig. 9 the validity of the scaling form given by Eq. (62) is demonstrated.

## X. CONCLUSIONS

In this paper, we have presented a detailed analysis of the dynamics of the contact process on annealed scale-free networks. Using stochastic differential equations for this dynamics, we have clarified the behavior of the model close to its critical point and, in particular, its finite-size scaling. Our results indicate that heterogeneous mean-field theory—strictly valid for infinite networks—is practically unobservable for the range of sizes that modern computers can reach. The dynamics is instead dominated by strong finite-size effects that give rise to nontrivial anomalous effects. Among them, it is worth noting that the scaling of several relevant quantities (like the order parameter close to the critical point or the surviving times of the dynamics, etc.) depends not

only on the system size $N$, as in regular lattices, but also on the upper cutoff $M$ of the scale-free degree distribution which, in general, diverges with the system size as $M \sim N^{1/\omega}$. The exponent $\omega$ is not fixed by the degree distribution alone and, in general, can take different values for different network models or even an arbitrary value that we can freely choose in annealed networks. This implies that the critical exponents of the dynamics are not universal but depend on the arbitrary value of $\omega$.

Our results allow us to understand the origin of the discrepancy between the phenomenological finite-size scaling theory proposed in Ref. [20] and the numerical results found in [24,25]. Indeed, the Langevin equation proposed in Ref. [20], Eq. (22), misses the crucial point that the coefficient $b$ is not a constant but depends on the system size, and grows with it. As a consequence, when the system is at its critical point and the concentration becomes small enough, the term $b\rho^2$ in Eq. (22) becomes more important than the term $d\rho^{\gamma-1}$, something that would not be possible if $b$ was a constant and $\gamma<3$. This change in the dominating term in Eq. (22) at low concentrations thus invalidates the FSS proposed in [20].

When $\omega<\gamma-1$ an additional interesting complication arises: the effective average cutoff of the degree distribution $k_c$ becomes $N^{1/(\gamma-1)}$, smaller than $M$, while its fluctuations diverge as $N$ grows. This means that, depending on the specific realization of the degree sequence, some outliers (i.e., nodes with a connectivity much larger than the effective average cutoff $k_c$) may appear. We have shown that a single outlier connected to a macroscopic portion of the system has the effect of introducing an apparent shift on the critical point position. The investigation of the role of outliers (and more in general the role of diverging fluctuations in the effective upper cutoff) in the contact process and other models is a very interesting avenue for further investigations. Notice that this case is the relevant one for simulations performed without fixing an explicit upper cutoff of the degree distribution, a very common habit.

Last but not least, we would like to stress that the theory and the simulations presented here give a complete understanding of the complex behavior of the contact process on *annealed* scale-free networks. Whether or not the same picture also holds for *quenched* topologies remains an open question calling for further work.

## ACKNOWLEDGMENTS

R.P.-S. and M.B. acknowledge financial support from the Spanish MEC (FEDER) under Project No. FIS2007-66485-C02-01 and No. FIS2007-66485-C02-02. R.P.-S. also acknowledges the hospitality of the Institute for Scientific Interchange Foundation, Turin (Italy), where part of this work was developed. R.P.-S. also acknowledges additional financial support through ICREA Academia, funded by the Generalitat de Catalunya.

## APPENDIX A: CALCULATION OF THE COARSE-GRAINED LANGEVIN EQUATION

The derivation of the Langevin equation that describes a general stochastic process $X(t)$ involves the evaluation of its infinitesimal moments. The first and second (variance) such moments inform us about the expected change in the process after an increment of time $dt$ and the variance of this expected change. More precisely, if we define the variable $\Delta X(t) \equiv X(t+dt)-X(t)$ [48], then the first infinitesimal moment is defined as

$$\Psi[x] = \lim_{dt\to 0} \frac{\langle \Delta X(t) | X(t) = x \rangle}{dt}. \tag{A1}$$

Analogously, the infinitesimal variance is defined as

$$D[x] = \lim_{dt\to 0} \frac{\langle [\Delta X(t)]^2 | X(t) = x \rangle}{dt}. \tag{A2}$$

The functions $\Psi[x]$ and $D[x]$ are called the drift and the diffusion term, respectively. The Langevin stochastic differential equation can then be written as

$$\frac{dX(t)}{dt} = \Psi[X(t)] + \sqrt{D[X(t)]}\xi(t), \tag{A3}$$

where $\xi(t)$ is a Gaussian white noise.

In our case, we are interested in writing a Langevin equation for the coarse-grained quantity $n_k(t)=\Sigma_{i\in k}\sigma_i(t)$. This is convenient for two main reasons. First, since it is the sum of almost (or totally) independent random variables, we expect the central limit theorem to hold. This guarantees that the corresponding noise in the Langevin equation is Gaussian and white. Second, in the thermodynamic limit, $n_k(t)/N$ can be safely assumed to be a continuous variable and, therefore, it is justified the use of (stochastic) differential equations.

To compute the infinitesimal first moment we write

$$\langle n_k(t+dt) | \boldsymbol{\Sigma}(t) \rangle = \sum_{i\in k} \sigma_i(t) \langle \zeta_i(dt) \rangle + [1-\sigma_i(t)] \langle \eta_i(dt) \rangle, \tag{A4}$$

where we have made use of Eq. (24). Finally, using the probability distributions Eqs. (25) and (26), we are led to

$$\langle n_k(t+dt) | \boldsymbol{\Sigma}(t) \rangle = n_k(t) + dt \Bigg( -n_k(t) + \lambda \sum_{k'} \frac{1}{k'} \sum_{i\in ks; j\in k'} \times a_{ij}[1-\sigma_i(t)]\sigma_j(t) \Bigg). \tag{A5}$$

Analogously, we can write an expression for the infinitesimal variance as

$$\langle n_k^2(t+dt) | \boldsymbol{\Sigma}(t) \rangle - \langle n_k(t+dt) | \boldsymbol{\Sigma}(t) \rangle^2 = dt \Bigg( n_k(t) + \lambda \sum_{k'} \frac{1}{k'} \sum_{i\in k; j\in k'} a_{ij}[1-\sigma_i(t)]\sigma_j(t) \Bigg). \tag{A6}$$

To derive the previous equation, we have taken into account that, since $\sigma_i(t)$ are binary variables taking only values 0 or 1, $\sigma_i^2(t)=\sigma_i(t)$ and that $\sigma_i(t)[1-\sigma_i(t)]=0; \forall\ t$. Terms of order $dt^2$ have also been neglected. Under the annealed approximation, we replace in Eqs. (A5) and (A6) the adjacency matrix $a_{ij}$ by its average value, Eq. (2), which allows us to

carry out the sums in Eqs. (A5) and (A6) and, finally, to obtain the Langevin equation Eq. (28).

## APPENDIX B: CALCULATION OF $\Theta[\rho]$ IN UNCORRELATED SF NETWORKS

Let us consider the definition of $\Theta[\rho]$ in Eq. (35), namely,

$$\Theta[\rho] = \sum_k \frac{kP(k)}{\langle k\rangle} \frac{\lambda k\rho/\langle k\rangle}{1+\lambda k\rho/\langle k\rangle}. \tag{B1}$$

The evaluation of this quantity in finite networks depends on the value of the particle density $\rho$. In particular, if $\rho \ll \langle k\rangle/\lambda k_c$, where $k_c$ is the network cutoff, then the denominator in Eq. (B1) can be approximated by unity, and we have

$$\Theta[\rho] \simeq \sum_k \frac{kP(k)}{\langle k\rangle}\frac{\lambda k\rho}{\langle k\rangle} = \frac{\langle k^2\rangle}{\langle k\rangle}\frac{\lambda\rho}{\langle k\rangle} = g\lambda\rho, \tag{B2}$$

where $g=\langle k^2\rangle/\langle k\rangle^2$. On the other hand, outside this region we must keep the full denominator in Eq. (B1). To estimate $\Theta$ in this case, we perform a continuous degree approximation, that is,

$$\Theta[\rho] = \int_m^{k_c} \frac{kP(k)}{\langle k\rangle}\frac{\lambda k\rho/\langle k\rangle}{1+\lambda k\rho/\langle k\rangle} = F\left[1,\gamma-2,\gamma-1,-\frac{\langle k\rangle}{\lambda\rho m}\right] - F\left[1,\gamma-2,\gamma-1,-\frac{\langle k\rangle}{\lambda\rho k_c}\right]\left(\frac{m}{k_c}\right)^{\gamma-2}, \tag{B3}$$

where $F[a,b,c,z]$ is the Gauss hypergeometric function. Using the asymptotic expansions of the hypergeometric function for small and large arguments [41], we can estimate the value of $\Theta$ in the domain $\langle k\rangle/\lambda k_c \ll \rho \ll 1$. Within such domain, the second term in Eq. (B3) becomes an asymptotically small constant as compared to the first term, which yields

$$\Theta[\rho] \simeq \Gamma(\gamma-1)\Gamma(3-\gamma)\left(\frac{\lambda\rho m}{\langle k\rangle}\right)^{\gamma-2}. \tag{B4}$$

.

## APPENDIX C: INITIAL TIME SCALE

To compute the initial time scale $t_\times$ needed to reach region I starting from an arbitrary initial condition $\rho_0$ at criticality, we consider Eq. (34) with the drift term given by Eq. (41) and $\Delta=0$, namely,

$$\frac{d\rho(t)}{dt} = -\frac{C(\gamma)}{\langle k\rangle^{\gamma-2}}\rho(t)^{\gamma-1}. \tag{C1}$$

The solution of this equation is

$$\rho(t) = \left(\rho_0^{2-\gamma} + \frac{(\gamma-2)C(\gamma)}{\langle k\rangle^{\gamma-2}}t\right)^{-1/(\gamma-2)}. \tag{C2}$$

The asymptotic state $\rho(t)\sim t^{-1/(\gamma-2)}$, independent of the initial condition, is reached for times $t$, such that

$$\frac{(\gamma-2)C(\gamma)}{\langle k\rangle^{\gamma-2}}t \gg \rho_0^{2-\gamma}, \tag{C3}$$

that is, for $t>t_\times$, with

$$t_\times = \frac{\rho_0^{2-\gamma}\langle k\rangle^{\gamma-2}}{(\gamma-2)C(\gamma)} = \frac{\rho_0^{2-\gamma}(\gamma-1)^{\gamma-2}}{(\gamma-2)^{\gamma-1}\Gamma(3-\gamma)\Gamma(\gamma-1)}, \tag{C4}$$

where we have used the definition of $C(\gamma)$ in Eq. (38) and $\langle k\rangle=(\gamma-1)m/(\gamma-2)$.

## APPENDIX D: SURVIVAL PROBABILITY EQUATION

Using standard techniques of stochastic processes theory, we can obtain the partial differential equation satisfied by the survival probability of the CP dynamics at criticality, starting from an initial concentration $\rho_0$, $S(t|\rho_0)$, namely [48],

$$\frac{\partial S(t|\rho_0)}{\partial t} = -\rho_0\Theta[\rho_0]\frac{\partial S(t|\rho_0)}{\partial\rho_0} + \frac{\rho_0}{N}\frac{\partial^2 S(t|\rho_0)}{\partial\rho_0^2}. \tag{D1}$$

This equation is the result of integrating the backward Fokker-Planck equation in the domain $\rho\in[0,1]$ and it should be solved with the initial condition $S(t=0|\rho_0)=1$ and boundary conditions

$$S(t|\rho_0=0)=0 \text{ and } \left.\frac{\partial S(t|\rho_0)}{\partial\rho_0}\right|_{\rho_0=1} = 0 \tag{D2}$$

which correspond to an absorbing boundary at $\rho=0$ and a reflecting one at $\rho=1$. The survival probability Eq. (23) can then be evaluated as

$$S(t) = S(t|\rho_0 = 1/N). \tag{D3}$$

We first start by evaluating the exponent $\delta$. To this end, it is only necessary to solve the problem in the thermodynamic limit $N\to\infty$. However, the above formulation is not the most appropriate for this purpose, since the solution must be evaluated at $\rho_0=N^{-1}$, that is, a value that depends on the size of the system. Therefore, we perform the change of variables

$$n_0 = N\rho_0, \tag{D4}$$

where $n_0$ is the initial number of active vertices, which is eventually set to $n_0=1$ and, therefore, is independent of the system size. Using this new variable, Eq. (D1) becomes

$$\frac{\partial S(t|n_0)}{\partial t} = -n_0\Theta\left[\frac{n_0}{N}\right]\frac{\partial S(t|n_0)}{\partial n_0} + n_0\frac{\partial^2 S(t|n_0)}{\partial n_0^2}. \tag{D5}$$

Notice that now the limit $N\to\infty$ can be taken in Eq. (D5). In this limit, the first term in the right-hand side of Eq. (D5) vanishes and the process becomes a purely diffusive one with multiplicative noise. The solution is

$$S(t|n_0) = 1 - e^{-n_0/t} \approx \frac{n_0}{t}. \tag{D6}$$

Setting finally $n_0=1$ leads to the exponent $\delta=1$ for any $\gamma$.

To evaluate the cutoff $t_c(N)$, we compute the second moment of the survival times, $T_2(n_0)$, starting from $n_0$ active sites. However, to compute $T_2$ we first need to compute the average surviving time $T_1(n_0)$. It is easy to see that $T_1(n_0)=\int_0^\infty S(t|n_0)$. Using this result in Eq. (D5), and assuming that trajectories never experience the type I drift, yields the following differential equation for $T_1(n_0)$:

$$\frac{d^2T_1(n_0)}{dn_0^2} - \frac{g}{N}n_0\frac{dT_1(n_0)}{dn_0} = -\frac{1}{n_0} \tag{D7}$$

with boundary conditions $T_1(0)=0$ and $T_1'(N)=0$. The solution of this problem is

$$T_1(n_0) = \sqrt{\frac{2N}{g}}\int_0^{n_0\sqrt{g/2N}} du\, e^{u^2}\int_u^{\sqrt{gN/2}}\frac{dt}{t}e^{-t^2}. \tag{D8}$$

When $N$ is very large, the upper limit in the first integral becomes very small. Therefore, we take the limit of the integrand when $u$ is close to zero, that is,

$$T_1(n_0) \simeq \sqrt{\frac{2N}{g}}\int_0^{n_0\sqrt{g/2N}} du(1+u^2+\cdots)(-\ln u+\gamma+\cdots) \tag{D9}$$

which finally leads to

$$T_1(n_0) \simeq -n_0\ln\left(n_0\sqrt{\frac{g}{2N}}\right). \tag{D10}$$

Similarly, the differential equation for $T_2(n_0)$ can also be obtained from Eq. (D5) as

$$T_2(n_0) = 2\int_0^\infty tS(t|n_0)dt. \tag{D11}$$

This results in the following differential equation [involving also $T_1(n_0)$]:

$$\frac{d^2T_2(n_0)}{dn_0^2} - \frac{g}{N}n_0\frac{dT_2(n_0)}{dn_0} = -\frac{2T_1(n_0)}{n_0}, \tag{D12}$$

which satisfies the same boundary conditions as $T_1(n_0)$. The solution of this equation is

$$T_2(n_0) = \frac{2N}{g}\int_0^{n_0\sqrt{g/2N}} du\, e^{u^2}\int_u^\infty G(t)e^{-t^2}dt, \tag{D13}$$

where

$$G(t) = \frac{2}{t}\int_0^t du\, e^{u^2}\int_u^\infty\frac{dq}{q}e^{-q^2}. \tag{D14}$$

In the limit of large $N$, this expression can be approximated as

$$T_2(n_0) = n_0\sqrt{\frac{2N}{g}}\int_0^\infty e^{-t^2}G(t)dt, \tag{D15}$$

proving then Eq. (46).

## APPENDIX E: PROBABILITY DENSITY FUNCTION FOR SURVIVING RUNS

At the critical point, the probability density $p(n,t|n_0)$ of the number of active vertices at time $t$ given that the process had $n_0$ active ones at time $t=0$ is ruled by a Fokker-Planck equation with a drift term $\Psi(n)=-n\Theta[n/N]$ and a diffusion coefficient $D(n)=2n$, that is,

$$\frac{\partial}{\partial n}\left(n\Theta\left[\frac{n}{N}\right]p(n,t|n_0)\right) + \frac{\partial^2}{\partial n^2}[np(n,t|n_0)] = \frac{\partial p(n,t|n_0)}{\partial t}. \tag{E1}$$

A direct substitution of Eq. (49) into Eq. (E1) leads to

$$\frac{\partial}{\partial n}\left(n\Theta\left[\frac{n}{N}\right]p_s(n,t|n_0)\right) + \frac{\partial^2}{\partial n^2}[np_s(n,t|n_0)] = \frac{\partial p_s(n,t|n_0)}{\partial t} + p_s(n,t|n_0)\frac{d\ln[S(t|n_0)]}{dt}. \tag{E2}$$

The density $p_s(n,t|n_0)$ has, by construction, a well-defined steady state, which we denote by

$$p_s(n) \equiv \lim_{t\gg 1} p_s(n,t|n_0), \tag{E3}$$

which is independent of the initial condition. By taking the limit $t\gg 1$ in Eq. (E2), we obtain

$$\frac{\partial}{\partial n}\left(n\Theta\left[\frac{n}{N}\right]p_s(n)\right) + \frac{\partial^2}{\partial n^2}[np_s(n)] = \kappa p_s(n), \tag{E4}$$

where

$$\kappa = \lim_{t\gg 1}\frac{d}{dt}\ln[S(t|n_0)]. \tag{E5}$$

Using the result given in Eq. (D6) we conclude that $\kappa=0$, meaning that $p_s(n)$ satisfies the potential solution of the Fokker-Planck equation [48]. We can then write that

$$\rho_s(0,N) \propto \frac{1}{N}\int_1^N e^{-\phi(n,N)}dn, \tag{E6}$$

with the effective potential

$$\phi(n,N) = \int\Theta\left[\frac{n}{N}\right]dn. \tag{E7}$$

As in the case of the function $\Theta$, the potential $\phi(n,N)$ takes a different functional form depending on the value of $n$. Direct integration of Eq. (37) gives

$$\phi(n,N) = \begin{cases} \dfrac{\lambda g}{2N}n^2, & n \ll \dfrac{\langle k\rangle N}{\lambda k_c}, \\ \dfrac{C(\gamma)}{\gamma-1}\left(\dfrac{\lambda}{\langle k\rangle N}\right)^{\gamma-2}n^{\gamma-1}, & \dfrac{\langle k\rangle N}{\lambda k_c} \ll n \ll N. \end{cases} \tag{E8}$$

At the critical point $\lambda=1$, we can use this result to write

$$\rho_s(0,N) \propto \frac{1}{N}\left(\int_1^{\langle k\rangle N/k_c} e^{-\phi_{\mathrm{II}}(n,N)}dn + \int_{\langle k\rangle N/k_c}^N e^{-\phi_{\mathrm{I}}(n,N)}dn\right), \tag{E9}$$

where the subscripts I and II refer to which type of potential is dominating the integral. In the limit $N\gg 1$, we can evaluate the contribution of each integral, leading to Eq. (51).

[1] S. N. Dorogovtsev, A. V. Goltsev, and J. F. F. Mendes, Rev. Mod. Phys. **80**, 1275 (2008).
[2] R. Albert and A.-L. Barabási, Rev. Mod. Phys. **74**, 47 (2002).
[3] S. N. Dorogovtsev and J. F. F. Mendes, *Evolution of Networks: From Biological Nets to the Internet and WWW* (Oxford University Press, Oxford, 2003).
[4] D. J. Watts and S. H. Strogatz, Nature (London) **393**, 440 (1998).
[5] A.-L. Barabási and R. Albert, Science **286**, 509 (1999).
[6] R. Cohen and S. Havlin, Phys. Rev. Lett. **90**, 058701 (2003).
[7] R. Pastor-Satorras and A. Vespignani, *Evolution and Structure of the Internet. A Statistical Physics Approach* (Cambridge University Press, Cambridge, U.K., 2004).
[8] R. Pastor-Satorras and A. Vespignani, Phys. Rev. Lett. **86**, 3200 (2001).
[9] A. L. Lloyd and R. M. May, Science **292**, 1316–1317 (2001).
[10] R. Cohen, K. Erez, D. ben-Avraham, and S. Havlin, Phys. Rev. Lett. **86**, 3682 (2001).
[11] D. S. Callaway, M. E. J. Newman, S. H. Strogatz, and D. J. Watts, Phys. Rev. Lett. **85**, 5468 (2000).
[12] R. Pastor-Satorras and A. Vespignani, Phys. Rev. Lett. **86**, 3200 (2001).
[13] M. Leone, A. Vázquez, A. Vespignani, and R. Zecchina, Eur. Phys. J. B **28**, 191 (2002).
[14] S. N. Dorogovtsev, A. V. Goltsev, and J. F. F. Mendes, Phys. Rev. E **66**, 016104 (2002).
[15] S. Dorogovtsev, A. Goltsev, and J. Mendes, Eur. Phys. J. B **38**, 177 (2004).
[16] L. K. Gallos and P. Argyrakis, Phys. Rev. Lett. **92**, 138301 (2004).
[17] M. Catanzaro, M. Boguñá, and R. Pastor-Satorras, Phys. Rev. E **71**, 056104 (2005).
[18] V. Colizza, R. Pastor-Satorras, and A. Vespignani, Nat. Phys. **3**, 276 (2007).
[19] C. Castellano and R. Pastor-Satorras, Phys. Rev. Lett. **96**, 038701 (2006).
[20] H. Hong, M. Ha, and H. Park, Phys. Rev. Lett. **98**, 258701 (2007).
[21] N. Goldenfeld, *Lecture Notes on Phase Transitions and the Renormalization Group*, Frontiers in Physics (Addison-Wesley, Reading, MA, 1992).
[22] J. Marro and R. Dickman, *Nonequilibrium Phase Transitions in Lattice Models* (Cambridge University Press, Cambridge, U.K., 1999).
[23] M. Ha, H. Hong, and H. Park, Phys. Rev. Lett. **98**, 029801 (2007).
[24] C. Castellano and R. Pastor-Satorras, Phys. Rev. Lett. **98**, 029802 (2007).
[25] C. Castellano and R. Pastor-Satorras, Phys. Rev. Lett. **100**, 148701 (2008).
[26] R. Pastor-Satorras, A. Vázquez, and A. Vespignani, Phys. Rev. Lett. **87**, 258701 (2001).
[27] M. A. Serrano, M. Boguñá, R. Pastor-Satorras, and A. Vespignani, in *Large Scale Structure and Dynamics of Complex Networks: From Information Technology to Finance and Natural Sciences*, edited by G. Caldarelli and A. Vespignani (World Scientific, Singapore, 2007), pp. 35–66.
[28] A. Bekessy, P. Bekessy, and J. Komlos, Stud. Sci. Math. Hung. **7**, 343 (1972).
[29] E. A. Bender and E. R. Canfield, J. Comb. Theory, Ser. A **24**, 296 (1978).
[30] B. Bollobás, Eur. J. Comb. **1**, 311 (1980).
[31] M. Molloy and B. Reed, Random Struct. Algorithms **6**, 161 (1995).
[32] M. Catanzaro, M. Boguñá, and R. Pastor-Satorras, Phys. Rev. E **71**, 027103 (2005).
[33] M. Boguñá and R. Pastor-Satorras, Phys. Rev. E **68**, 036112 (2003).
[34] S. N. Dorogovtsev, J. F. F. Mendes, and A. N. Samukhin, Phys. Rev. Lett. **85**, 4633 (2000).
[35] S. Gil and D. Zanette, Eur. Phys. J. B **47**, 265 (2005).
[36] D. Stauffer and M. Sahimi, Phys. Rev. E **72**, 046128 (2005).
[37] S. Weber and M. Porto, Phys. Rev. E **76**, 046111 (2007).
[38] I. V. Belykh, V. N. Belykh and M. Hasler, Physica D **195**, 188 (2004).
[39] S. N. Dorogovtsev and J. F. F. Mendes, Adv. Phys. **51**, 1079 (2002).
[40] M. Boguñá, R. Pastor-Satorras, and A. Vespignani, Eur. Phys. J. B **38**, 205 (2004).
[41] *Handbook of Mathematical Functions*, edited by M. Abramowitz and I. A. Stegun (Dover, New York, 1972).
[42] M. Boguñá, R. Pastor-Satorras, and A. Vespignani, in *Statistical Mechanics of Complex Networks*, edited by R. Pastor-Satorras, J. M. Rubí, and A. Díaz-Guilera, Lecture Notes in Physics vol. 625 (Springer-Verlag, Berlin, 2003).
[43] H. E. Stanley, *Introduction to Phase Transitions and Critical Phenomena* (Oxford University Press, Oxford, 1971).
[44] M. Boguñá and R. Pastor-Satorras, Phys. Rev. E **66**, 047104 (2002).
[45] V. Privman, *Finite Size Scaling and Numerical Simulation of Statistical Systems* (World Scientific, Singapore, 1990).
[46] D. H. Zanette, Phys. Rev. E **64**, 050901(R) (2001).
[47] P. R. A. Campos, V. M. de Oliveira, and F. G. Brady Moreira, Phys. Rev. E **67**, 026104 (2003).
[48] G. W. Gardiner, *Handbook of Stochastic Methods for Physics, Chemistry and the Natural Sciences* (Springer-Verlag, Berlin, 2004).
[49] V. Sood and S. Redner, Phys. Rev. Lett. **94**, 178701 (2005).